Final Report

15 November 1968 to 15 December 1969

TOTAL ENERGY DISTRIBUTION MEASUREMENTS OF FIELD EMITTED ELECTRONS

By

L. W. Swanson
L. C. Crouser

Prepared for

Headquarters
National Aeronautics and Space Administration
Washington, D. C.

December, 1969

CONTRACT NASw-1516

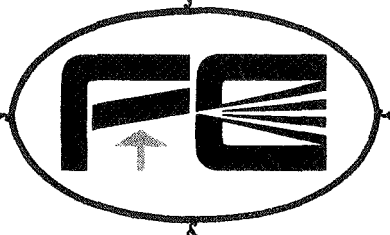

Field Emission Corporation

McMinnville, Oregon

Requests for copies of this report should be referred to

National Aeronautics and Space Administration
Office of Scientific and Technical Information
Attention: AFSS-A
Washington, D.C. 20546

Final Report

15 November 1968 to 15 December 1969

TOTAL ENERGY DISTRIBUTION MEASUREMENTS OF FIELD EMITTED ELECTRONS

By

L. W. Swanson
L. C. Crouser

Prepared for

Headquarters
National Aeronautics and Space Administration
Washington, D. C.

December, 1969

CONTRACT NASw-1516

PREFACE

This report describes work being performed under support from NASA, Headquarters, Washington, D. C. under contract NASw-1516. Our primary objective during this period was to explore the total energy distribution (TED) measurements of field emitted electrons in regards to the effect of adsorption. In particular we have attempted to understand the cause of the structure observed on the TED when polyatomic molecules are adsorbed at the surface. In addition, we have continued studies of the structure in TED curves from clean surfaces.

I. The Effect of Polyatomic Adsorbates on the Total Energy Distribution of Field Emitted Electrons

INTRODUCTION

Experimental studies by Lambe and Jaklevic[1] of MOM tunneling junctions and Thompson[2] of Schottky barrier MS diodes have shown that tunneling electrons are inelastically scattered by polyatomic molecules absorbed in the diode interface. This particular electron-phonon interaction mechanism was revealed experimentally by an enhancement in the diode conductance at various diode bias voltages characteristic of the vibronic spectra of the adsorbed molecules. Thus, a novel molecular spectrometer covering a wide range of wavelengths from the microwave to the visible and possessing a resolution of the order of 5 kT was unveiled by these findings.

Another mechanism by which adsorbates perturb the tunneling electrons is through a transmission resonance caused by wave mechanical interference effects due to the presence of discrete atomic potentials lying outside the main electronic charge cloud of the bulk metal. This mechanism was analyzed mathematically by Duke and Alferieff[3] who employed a one-dimensional pseudopotential model. According to their results atomic or molecular levels of an adsorbed particle lying within the conduction band provide windows of enhanced electron tunneling which can be most readily detected by analyzing the total energy distribution (TED) of the emitted electrons.

The prospect of detecting either or both of these effects on field emitted electrons at the metal-vacuum interface has prompted us to investigate the TED of vacuum field emitted electrons from substrates with chemisorbed monomolecular films. Useful information regarding the perturbation of the electronic and/or vibronic levels of the adsorbate by the adsorption act is potentially accessible from such measurements. In addition, the possibility of elucidating certain aspects of surface catalytic mechanisms in the chemisorption process portends to be a technologically useful derivative of these measurements.

Initial efforts in this direction using phthalocyanine (pht), primarily because of its large size and ease of handling in high vacuum, have been reported.[4] In this report further results and interpretations of the phthalocyanine work are given along with preliminary results from pentacene adsorbed on the (310) plane of W. Evidence that both electronic and vibronic spectral information can be obtained by energy analysis of the field emitted electrons transmitted through large organic molecules is given.

THEORETICAL CONSIDERATIONS

A theoretical description of the effect of adsorbed molecules on the energy distribution of field emitted electrons with respect to tunnel resonance[3] and electron-phonon interaction[1] has been given. As pointed out in a previous report the large cross sectional area of these organic molecules should enhance detection of low transition probability phenomena.[4]

In addition to tunnel resonance and electron-phonon interaction, a third possibility to be considered is electron-electron interaction. Organic molecules such as those studied here possess low lying electronic states, e. g. , singlet and triplet, which can be excited by the tunneling electrons. In other words we have the possibility of elastic scattering of the tunneling electrons through tunnel resonance and/or inelastic scattering through two possible mechanisms, electron-phonon and electron-electron interactions.

It would be helpful to summarize the qualitative theoretically expected experimental manifestations of the above mentioned mechanisms. Basically there are four experimental observables which can be compared with experimental predictions; they are as follows:

1) the overall shape of the TED
2) the intensity and displacement of the new structure in the TED due to the adsorbate
3) the effect of electric field and temperature on 1) and 2)

First let us examine in qualitative fashion the expectations of the above consideration for tunnel resonance. Based on the present physical picture

(see Fig. 1) in which a Lorentzian shaped virtual electronic level in the adsorbate is positioned at Δ (energy relative to the Fermi level), Gadzuk has shown that the TED including transmission resonance can be expressed as

$$J_{tr}(\varepsilon) = J(\varepsilon)\left[1 + \frac{T_{tr}^2}{(\varepsilon-\Delta)^2+\Gamma^2} - \frac{2(\varepsilon-\Delta)T_{tr}}{(\varepsilon-\Delta)^2+\Gamma^2}\right] \quad (1)$$

where T_{tr} is the ratio of the adsorbate coated to clean tunneling probabilities and Γ is the half width of the broadened adsorbate level which increases with decreasing metal-adsorbate distance. As pointed out previously[5], the first term on the right hand side is the direct tunneling expression. The second term is the resonance tunneling factor which assumes a Lorentzian shaped broadened adsorbate level. The third term is an interference term between the direct and indirect channels. Thus the resonance peak will have a skewed Lorentzian shape centered on Δ.

A word concerning the magnitude of T_{tr} should be given. Crudely speaking T_{tr} is the ratio of the adsorbate coated to bare surface tunneling probability where the adsorbate modifies the bare surface potential by the presence of the adsorbate potential well of width w and x_o from the surface as depicted schematically in Fig. 1. From WKB considerations of tunneling through a triangular barrier, the tunneling amplitude is proportional to $\exp\{-c\int_{x_1}^{x_2}[\phi(x) - E_x]^{1/2}dx\} = \exp[-c(E_f + \phi - E_x)^{3/2}/F]$. Assuming the adsorbate modifies the barrier by cutting out a square well of width w and height $E_x - Fx$, the qualitative expression for T_{tr} becomes

$$T_{tr} \cong F(\varepsilon) \frac{\exp -c\,[(E_f + \phi - E_x)^{3/2}/F - (\phi - \varepsilon_x - Fx_o)^{1/2} w\,]}{\exp\,[-c(E_f + \phi - E_x)^{3/2} / F]} \tag{2}$$

$$= F(\varepsilon)\, \exp\,[\, c\,(\phi - \varepsilon_x - Fx_o)^{1/2} w\,].$$

has units of energy and where $F(\varepsilon)$ is a slowly varying function of ε whose magnitude is the order of unity and where $c = 2\,(2m)^{1/2}/h$. For $\phi = 4.5$, $E_x = -0.5$, $F = 0.3$ V/Å and $w = 2$ Å, $T_{tr} = 18$. Also note that T_{tr} increases as the well depth increases and that $J(\varepsilon)$ goes to zero for $\varepsilon > o$; thus for $\Delta > o$ little effect will be observed on $J(\varepsilon)$.

According to a highly simplified model[3] the virtual level Δ will shift downward with field F according to Fx_o. However, upon including the image potential term, polarization of the atom by the electric field and Stark shifts, a more complicated field shift of the resonance level may occur in practice. Assuming no temperature dependent change in the adsorbate position x_o, no particular effect of temperature on the shape or displacement of the tunnel resonance peak is expected.

Next, let us examine the effect of electron-phonon interactions of the tunneling electrons. Electrons tunneling from the metal at energy level ε inelastically scattered by a phonon excitation $h\nu$ will ultimately tunnel through a separate channel at $\varepsilon - h\nu$ (see Fig. 2). Thus, the TED shape at the Fermi level will be replayed at $\varepsilon - h\nu$ reduced by a probability factor T_{ep} for an inelastic interaction. In this case the expression for the TED can be qualitatively expressed as

$$J_{ep}(\varepsilon) = J(\varepsilon)(1 - T_{ep}) + J(\varepsilon + h\nu) T_{ep} g_p(\varepsilon - h\nu) \quad (3)$$

where the first term represents the reduction in the unperturbed TED due to electrons which channel separately at $\varepsilon - h\nu$. The factor $g_p(\varepsilon - h\nu)$ represents the line shape broadening due to a possible finite continuum of phonon levels or lifetime effects.

In general the shape of the TED structure due to electron-phonon interactions will be a reduced replica of the unscattered TED at the Fermi level. A theoretical description of this has been given elsewhere for the vacuum field emission case and for the closely analogous tunnel diode configuration. If the transition is sharp the shape factor $g(\varepsilon - h\nu)$ will be near unity and the leading edge shape of the electron-phonon transition will be due to the temperature or resolution broadening of the Fermi level electrons. Thus, TED structures due to e-p transitions should exhibit a leading edge which broadens with temperature.

A Stark splitting of the electron-phonon transitions can be envisioned in the case of degenerate vibrational rotational or bending modes. However, a qualitative prediction as to the magnitude of such field effects on the electron-phonon interaction is not possible from the present theoretical status. As best the effect of field on e-p transitions is expected to be smaller than for tunnel resonance. This is born out by the experimental results of Lambe and Jaklevic[1] which show that the tunnel electron spectra of complex molecules is strikingly similar to the corresponding field free infra-red spectra.

The magnitude of the electron-phonon interactions will obviously be proportional to the oscillator surface density as well as T_{ep}. In general $T_{ep} \propto < m \mid p_z \mid 0 >$ where p_z is the dipole moment perpendicular to the surface and $< m \mid p_z \mid 0>$ is the matrix element coupling the ground vibrational state m = 0 to m. As pointed out by Lambe and Jaklevic[1] this technique may also be useful in detecting Raman spectra.

Finally, let us consider the electron-electron (e-e) interaction. Our focus here is upon the possibility of the tunneling electron to excite the adsorbate electrons in the upper filled molecular orbitals to low lying excited states as depicted in Fig. 3. Since the tunneling electrons have several volts of energy relative to the uppermost filled state of the adsorbate molecules, excitation to levels a few volts above the ground state is possible. Cross sections for π orbital electrons should be of the order of the molecular dimensions for the conjugated molecules being examined here.

Qualitatively speaking, the expression describing the TED structure due to e-e interactions should have the following form

$$J_{ee}(\varepsilon) = J(\varepsilon)\,(1 - T_{ee}) + J(\varepsilon + h\nu)\, T_{ee}\, g_e(\varepsilon - h\nu). \qquad (4)$$

It will be noticed that the form and symbol meanings of Eq. (4) are identical to Eq. (3). The shape factor $g_e(\varepsilon - h\nu)$ originates from the same considerations which led to the Lorentzian shape of the broadened adsorbate level in Eq. (1). We anticipate Γ to be rather small for deep lying levels where the metal-adsorbate orbital overlap will be small. If Γ is sharp, i.e., $\Gamma < kT$ the shape of the Fermi level TED is simply replayed at $\varepsilon - h\nu$ as in the case of

electron-phonon ineteraction. We therefore expect temperature broadening to be manifest in the e-e transition where $\Gamma < kT$.

The effect of field on the e-e peak position cannot be ascertained from our present understanding; however, it will be proportional to the difference between the field shift in the ground and excited state levels. Stark shifts for these highly polarizable molecules are likely to be important.

From elementary considerations two Stark shifts can be identified for electronic transitions. In the case of a non-degenerate state one may observe a quadratic shift in an energy level E_g with field.

$$E_g = \frac{eF^2\alpha}{2} \cdot \tag{5}$$

It is actually the difference between the field shift of two levels E_g and E_g' that is observed in a transition. For $\alpha = 50$ Å and $F = 0.3$ V/Å the value of $\Delta E_g/\Delta F = 0.5$ Å. Thus, the quadratic Stark shift will be quite small for even highly polarizable molecules.

A linear Stark shift arises from the action of an electric field on a degenerate energy level E_o. The energy level will then split into two levels given by

$$E_n = E_o \pm eF\,|Z|_{12} \tag{6}$$

where $Z_{12} = \int U_1^* Z_{12} U_2\, dx$. In essence Z_{12} is roughly the mean difference in atomic size in states 1 and 2. For the hydrogen atom one can show that $Z_{12} \cong 3a_o$, where a_o is the Bohr radius. Thus, for the hydrogen atom $\Delta E_n/\Delta F = 1.5$ Å. Clearly, the linear Stark effect is expected to pre-

dominate from these elementary considerations.

By way of summary, a comparison between Eq. (1) depicting elastic scattering and Eq. (3) and (4) depicting inelastic scattering yields the following expectation: the shape of the subsidiary TED structure in the case of elastic scattering is Lorentzian and unrelated to the Fermi level emission peak; the opposite is generally expected to be the case for inelastic scattering, whether electron-electron or electron-phonon. In addition, elastic tunnel resonance and electron-electron scattering should exhibit a larger $\Delta E/\Delta F$ than an electron-phonon interaction.

EXPERIMENTAL

Experimental details of the van Oostrom analyzer employed in this work have been described elsewhere[4]. Because of the relative insensitivity of this analyzer to the tip position we found it to be more versatile than the concentric sphere design described previously.

In order to facilitate the data reduction a Princeton Applied Research HR-8 lock-in amplifier has been incorporated into the system. This instrument allows electronic differentiation of the probe current, that is dI/dV, to be accomplished. Briefly a 1000 hz signal is impressed on the probe current I by modulating the bias voltage with a 10 to 20 mV signal. The output dI/dV is plotted vs V_{bias} on an x-y recorder. The derivative can be taken electronically for probe current levels above 5×10^{-12} Å. In most cases the 300 msec integrator time constant selector of the HR-8 is used. This allows the V_{bias} sweep of ~3V to be made in ~30 sec.

Both pentacene and metal free phthalocyanine were thoroughly outgassed

prior to being put into resistively heatable platinum buckets. Anthracene was distilled into a break off seal from which it was subsequently sublimed onto the emitter. Controlled deposition of molecules onto the tip could therefore be accomplished. The presence of an individual molecule(s) in the probe area could be ascertained by noting the sharp rise in probe current due to the adsorption of a molecule. By observing the pattern and electron current, the adsorbed molecule could be positioned in the center of the probe by magnetic deflection. This was done more effectively in the case of the pentacene results. Frequently the molecule would change its emission characteristics during TED measurements or disappear by diffusion or desorption from the probe hole region.

From the present state of knowledge one cannot be sure each adsorption event concerns an individual molecule or a higher order conglomerate of molecules. Both pentacene and phthalocyanine are conjugated planar molecules. Pentacene and anthracene consist of a linear chain of 5 and 3 fused benzene rings respectively and contain only C-C and C-H bonds where each C atom is sp^2 hybridized. Phthalocyanine is a four-fold symmetrical molecule approximately 10 by 10 $\mathring{A}$ and pentacene is an oblong molecule roughly 4 by 12 $\mathring{A}$.

It is well known that large organic molecules[8] frequently produce characteristic molecular patterns when adsorbed on a field emitter. These molecular patterns are usually a single spot, a doublet or quadruplet set of spots. With the tube geometry employed, the molecular pattern frequently encompassed the total probe area. This was particularly true with the pentacene results.

RESULTS

Phthalocyanine

Although the TED results of phthalocyanine on W and Mo have been previously reported[4], we shall summarize the pertinent results here. Figs. 4 to 15 show TED spectra for phthalocyanine on various planes of W and Mo at 77°K. The experimental details have been discussed elsewhere.[4] For the most part, phthalocyanine was deposited onto the tip at 77°K. Removal of the phthalocyanine was effected by thermal heating, thus the substrate surface was carbon contaminated for the most part.

By monitoring the emission current while the molecules of phthalocyanine were being deposited one could detect the deposition of a single molecule (assuming monomolecular vaporization) of phthalocyanine. Often the probe current was very noisy and erratic due to what appeared to be thermally or field induced random steric changes in the adsorbate-substrate configuration. These steric changes of the adsorbate frequently altered the TED structure. In addition, a higher frequency noise current whose amplitude appeared to increase with temperature was usually observed. Thus, lowering the temperature to 20°K (liq. H_2) may reduce some of this undesirable noise problem.

It was observed that the noise current amplitude Δ I was not only a function of temperature but was also directly proportional to I. This suggests that the electrons which traverse the ad-molecule deposit energy in vibrational or some other thermal modes of the molecule which cause a fluctuating effective dipole moment. The latter in turn modulates the cur-

rent through the sensitive dependence of I on the work function.

The different TED curves shown in Figs. 4 to 13 arise from separate depositions of phthalocyanine onto the substrate. Unfortunately in the particular analyzer employed here, the electron beam could not be easily deflected so as to position the probe hole over a single molecular spot; thus, some of the difficulty in reproducing a given TED structure may have been due to two or more molecules with different steric configurations contributing to the total TED. This limitation was eliminated in the pentacene work reported below by employing a tube with electrostatic deflection plates. A further complication possibly hindering reproducibility was the continuing carburization of the surface due to thermal cracking of the phthalocyanine molecules during cleaning. This undesirable feature too was eliminated in the pentacene results by low temperature field evaporation cleaning of the surface.

In summarizing the phthalocyanine TED curves, we have also plotted the shift in the peak relative to the Fermi peak as a function of applied field. Because of some uncertainty in calculating field strengths due to carbon contamination, some error may be contained in the exact relative positioning on the F axis. Generally speaking results on a given plane should have greater relative significance. In the caption we have included when available the ratio of the adsorbate to clean probe current increase I_a/I_c, the clean work function ϕ_c, the work function change $\Delta\phi$ and the change in pre-exponential factor of the Fowler-Nordheim (FN) equation; that is

$$B = \ln A - \ln A_c$$

where A_c is the clean value of the FN equation pre-exponential.

We should hasten to point out that parameters obtained from FN analysis of I(V) data where TED structure is present must not be equated with their original physical meanings. For example, FN plots are frequently non-linear as shown in Fig. 16 which goes with the TED shown in Fig. 15.

The TED curves have been replotted from the original data and normalized to put the peak maximum at unity. Clean TED's are shown in most cases for comparison purposes. Two TED's at different field strengths are plotted for comparison for each TED structure observed. The maximum number of new peaks observed in the TED structure due to adsorption was three.

Fig. 14 shows a result obtained only in a few cases in which a large emission peak was observed above the Fermi level, E_f. In another instance, peaks occurred both at 900 mV above E_f and -575 mV below E_f. In the latter case, the -575 mV peak was much smaller than the 900 mV one. Unfortunately, the field shift for these peaks was not obtained.

The two TED curves in Fig. 6 are from two different depositions. The TED curves of Fig. 12 and 13 are derived from the same deposition; apparently, the molecule underwent a spontaneous steric change which gave rise to another TED structure.

Pentacene

The pentacene results were obtained on a <310> W emitter which was cleaned by field evaporation. Subsequent removal of pentacene was carried out by field desorption so as not to alter the substrate surface

through carburization. The deposition of pentacene and the measuring of the TED curves were always performed at 77°K. Noise problems were similar to the phthalocyanine studies.

The summary of the pentacene results are given in Figs. 17 to 20. These results were all obtained from singlet molecular patterns. Of particular interest are the peaks in Fig. 20 appearing nearly 3 V below the Fermi level. Fig. 21 summarizes the field shift of the peaks observed in the pentacene results. The results of investigating the temperature effect on the TED structure is shown in Fig. 22. Unfortunately, it was extremely difficult to measure the TED curves above 77°K because of excessive noise and irreversible changes in the TED structure. Fig. 23 is a replot of the TED structure shown in Fig. 19 for the purpose of illustrating an unusual increase in the Boltzman tail as the field is increased. The latter was an infrequent occurrence that was not observed with phthalocyanine.

DISCUSSION

The first and foremost objective of this research was to determine which of the three possible mechanisms discussed above are operative. Clearly, the direction of future work and utility of this technique as a surface spectrometer cannot be determined until a clear understanding of the mechanism is ascertained. Let us first consider the two possible mechanisms, inelastic or elastic scattering.

One of the important differences between elastic processes occurs in the ratio of $J(\varepsilon = \Delta \text{ or } h\nu)/J(\varepsilon = 0)$. That is to say, the amount of emis-

sion from the subsidiary peaks relative to the Fermi level emission is different for the two processes. For inelastic transmission resonance we obtain from Eq. (1)

$$J(\Delta)/J(0) = e^{\Delta(F)/d}(1 + T_{tr}^2/\Gamma^2)/(1 + \frac{T^2_{tr}}{\Delta^2+\Gamma^2} - \frac{2\Delta\ Ttr}{\Delta^2 + \Gamma^2}) \qquad (7)$$

where $\Delta(F)$ varies approximately linearly with F. Similar consideration leads to the following expression in the case of inelastic scattering

$$J(h\nu)/J(0) = e^{h\nu(F)/d} + T_{in}\ g(0)/(1 - T_{in}) \qquad (8)$$

where again $h\nu$ (F) varies linearly with F (as observed experimentally) and T_{in} is the inelastic transition probability. One of the important consequences of the Eqs. 7 and 8 is in regards to the expected magnitude of the subsidiary peak(s) relative to the Fermi level emission. For example, since $\Delta(F)$ is always negative and equal to or greater than d and since the factor to the right of $e^{\Delta(F)/d}$ is of the order of unity it follows that $J(\Delta)/J(0) << 1$; this of course becomes increasingly true as $\Delta(F)$ increases negatively. On the other hand, for inelastic scattering, although $e^{h\nu(F)/d}$ may be small because of a large negative value of $h\nu$ (F), it follows that $J(h\nu)/J(0) \gtrsim 1$ provided T_{in} is near unity. Also in this case, the value of $J(h\nu)/J(0)$ should be relatively independent of F. Thus, we may expect the relative size of $J(\varepsilon)$ at the Fermi level to the subsidiary peak to give an important clue as to the mechanism.

In the case of elastic scattering $J(\Delta)/J(0)$ can either increase (if Δ_o

is negative or below the Fermi level) or decrease (if Δ_o is positive) with F. If Δ is negative, the value of $J(\Delta)/J(0)$ will generally be small, the order of unity or less. We can summarize by noting that $J(\Delta)/J(0) \propto e^{\pm \Delta_o/CF}$ whereas $J(h\nu)/J(0) \propto e^{-h\nu_o/CF} + B$ where the constant B can be large compared to $e^{-h\nu_o/CF}$.

We should point out that the derivation of the above equation is based on the assumption that all the electrons entering the probe area pass through the molecule. In the event this assumption does not hold, the terms on the right hand side of Eqs. (1), (3) and (4) must be multiplied by the appropriate fractional area. On the basis of the cross sectional area of the two molecules studied and the overall magnification, it follows that the projected molecular pattern should cover the probe area as generally confirmed from pattern observation.

The ratio of the subsidiary peak heights to that at the Fermi level is greater than unity in Figs. 4 and 5 for pht. on Mo (110). Also the shift in the peaks with field is relatively small. These observations fit the expectations for the case of electron-phonon inelastic scattering.

There are two additional peaks which have small values of dE (Displ.)/dF. The TED curve in Fig. 6 with dE/dF = 1 Å exhibits a $J(\Theta h\nu)/J(0)$ which is greater than unity. Also the peaks in the Fig. 7 curve with dE/dF = 0.5 Å has $J(h\nu)/J(0)$ = const. independent of F. For the most part, the peaks with small displacements and small dE/dF were found on the 110 plane of either W or Mo.

Unpublished studies of the fine structure associated with pht adsorbed

in a tunnel diode by Lambe and Jaklevic shows structure in the 50 to 80 mV energy loss region. Higher energy transitions were not investigated. Infrared studies[9-11] show strong absorption in the 90 mV region that is attributed to a C-H bending mode. Several strong IR peaks were also observed in the 125 to 200 mV region. The TED peaks observed in this work at 90 and 150 mV (at 0.35 V/Å) may well correspond to the IR vibronic spectra. The TED peak at 250 mV (the middle peak of Fig. 7) also has characteristics of an electron-phonon interaction, but has no corresponding analogue in the IR spectra.

The two TED curves shown in Fig. 6 for pht on W (111) also exhibit small values of dE/dF, except for the lower field region of one which has a steeper portion segment. Both of these TED curves show ratios of J(hν or Δ)/J(0) which are nearly independent of F; this observation lends support to an electron-phonon description, i.e. Eq.(8) in which the second term is larger. The rather broad leading edge is somewhat puzzling to explain in terms of a strictly electron-phonon interaction and must be ascribed to phononic level broadening. This Fig. 6 shaped TED was only observed on W (111).

As mentioned previously the middle peak in the TED curve of Fig. 7 fits an electron-phonon interaction in view of the constant J(hν)/J(0) independent of F and the small dE/dF. In contrast the high energy peak shifts markedly with F (i.e., large dE/dF) and the shape is similar to the Fermi level peak. Thus, this transition is more in line with an inelastic process, but more likely an electron-electron interaction because of the large value of dE/dF.

Fig. 8 is another double peaked structure obtained from W (110) in

which both peaks are larger than the Fermi level emission, have nearly the same shift with field and are separated by 400 mV. The relative positions of the peak heights vary only slightly with field strength. These observations lend support for an electron-electron interaction. Conceivably, the double peak involves a combination electronic transition and vibrational overtone excitation. Interestingly, there is a strong IR absorption at 400 mV which corresponds to a N-H vibration.

The results of Figs. 9 and 10 on Mo (110) and W (111) both have a large and identical value of dE/dF but separated by 200 mV. The extremely steep leading edge and overall similarity of shape to the Fermi level emission suggests a sharp electron-electron transition. On this basis the very narrow half width of curve 2 arises from the low field strength since for the Fermi level emission half width is proportioned to F. Clearly, in this case T_{in} must be the order of unity.

The TED curves of Figs. 11 and 12 are from the same molecule which spontaneously changed its TED structure during the course of the measurement. We notice that in each case the lowest transition overlaps the Fermi level emission at low fields. All peaks are strongly sensitive to field and the low energy peak coincides in both cases. The separation of peaks in Fig. 11 is ~300 mV whereas in Fig. 12 the separation is of the order of 200 mV. Here again it is possible that the lowest peak is due to an electron-electron interaction while the higher transitions represent combination electron-vibronic and/or overtone transitions.

The Fig. 13 results on W (111) show two subsidiary peaks which have

distinctly different field shifts and which are both greater than the Fermi level emission. The relative peak heights and shapes are reasonably independent of field strength although the low energy transition has a broader half width. It is again tempting to suggest that the two transitions are both due to an inelastic scattering process. The high energy transition is the order of 1 volt in the field range investigated and has the characteristics of an electron-electron excitation of the molecule to a non-broadened electronic level. Comparing the Fig. 8 and 13 results shows that the low energy transition peaks possess nearly identical dE/dF and shapes. In both instances the low energy peak exhibits a broader half width. A similar shaped peak with the same dE/dF is shown in the Fig. 7 Mo (110) results.

A summary of the field dependence of the peak positions in Figs. 4 to 14 clearly shows 3 classes of relations. One group shows a large slope, between 3.9 and 5.0 Å; another group exhibits a value around the 2.0 Å, while the rest exhibit slopes less than 1 Å. Those in the latter group are best explained in terms of electron-phonon enteractions as mentioned earlier. The group of peaks with the 3.9 to 5.0 Å and 2.0 to 2.2 Å slopes are best explained in terms of electron-electron excitation. A difference in the orbital steric configuration of the electronic states involved would be manifested in Eq. (6) as an effective difference in $|Z|_{12}$ and could account for the different values of $d\,\Delta E/dF$. The parallel vertical displacements of those peaks with nearly identical $d\,\Delta E/dF$ may be due to combination electronic-vibronic transitions. In other cases a multiplicity of steric possibilities may alter the effective field strength and thereby cause horizontal displacements in

the ΔE vs F curves.

Striking evidence that some long lived excited states are involved in the phthalocyanine results is given in the Fig. 14 results. Here a peak occurs 950 mV above and 1200 mV below the Fermi level for F = 0.39 V/Å. This sort of result was observed only in a few cases of phthalocyanine depositions. In another result a peak was observed 575 above and 900 mV below the Fermi level for F = 0.32 V/Å; however, the 575 mV peak was considerably smaller in this case. A possible explanation of these results ia an Auger type mechanism in which an excited electronic state of the molecule is sufficiently long lived (compared to the interelectron tunneling time) that a subsequent tunneling electron stimulates the de-excitation. The latter electron takes up the de-excitation energy in the process and appears above the Fermi level. That this result was not frequently observed is indicative of the fact that for the most part de-excitation occurs faster than interelectron tunneling time. The fact that the upper peak displacement from the Fermi level is less than the lower peak displacement by 250 mV may stem from the fact that stimulated de-excitation occurs to a metastable, rather than the original ground state.

Figs. 15 and 16 show a TED and a corresponding Fowler-Nordheim plot. In view of the non-linear nature of the plot one should exercise considerable caution in attributing the usual physical significance to the Fowler-Nordheim constants.

Figs. 17 to 20 are TED's obtained from various depositions of pentacene (pent) on W (310) at 77°K. These results were obtained from singlet

molecular patterns. The results are similar to the phthalocyanine results except for the appearance of a peak at the astonishing displacement of ~3 eV below the Fermi level as observed in Fig. 20. Excluding Fig. 19 all the TED's exhibit relatively large peaks compared to the Fermi level emission. For the most part the relative peak heights are independent of field strength as observed with the phthalocyanine results.

The Fig. 17 results show three peaks, two of which exhibit nearly identical field shifts. The upper peak exhibits a very broad half width and a small field dependency and could best be ascribed to a tunnel resonance mechanism. The lower peak appears to be an electronic transition with a possible vibronic overtone.

The transitions observed in Figs. 18 to 20 are also best explained in terms of an electron-electron interaction. The peak 3 eV below the Fermi level in Fig. 20 must be due to an electron-electron transition in view of the exceedingly low value of $J(\Delta)/J(0)$ for electrons 3 eV below the Fermi level according to Eq. 3.

A summary of the pentacene results shown in Fig. 21 shows an interesting 150 mV separation between the 4 peaks observed with the 3.3 to 3.6 Å slope. As pointed out before, the vertical separation between these peaks is either due to a difference in true field at the molecule, or random spacial variations in the adsorbed state of the molecule which alter the electronic transition selection rules.

As mentioned earlier elastic scattering due to tunnel resonance should be temperature independent in first order; whereas inelastic tunneling peaks

should exhibit a temperature broadening of the leading edge. Fig. 22 shows the results of an experimental attempt to examine the temperature effect on a TED peak due to pentacene. Many attempts were unsuccessful due to irreversible changes in the TED structure upon heating. Thus, the Fig. 22 results, which should be taken as tentative until more concise results are obtained, show a definite broadening of the leading edge of the TED peak below the Fermi level. This result as it stands however supports the electron-electron excitation explanation. The very large half width of the Fig. 22 curve suggests an unusually large degree of broadening of the levels involved .

Fig. 23 is simply a replot of the Fig. 19 results on a semi-log graph to emphasize the unusual broadening of the leading edge as the field is increased. The degree of broadening corresponds to a few hundred degrees temperature change. Since it is unlikely that the metallic electrons are heated even locally to such temperatures by emission heating, the broadening must be due to an electron-phonon interaction for electrons emitted at the Fermi level. Apparently in this case the rapid electronic de-excitation has resulted in a sufficiently long-lived phononically excited molecule that tunneling electrons couple to the phonon modes so as to take up phononic energy. The increase in the phonon spread with current must simply reflect a "hotter" molecule. We should note that this sort of broadening of the Boltzman tail was not a general occurrence.

In contra-distinction to the phthalocyanine results, we have no observation of direct electron-phonon excitation of pentacene. This may

be a result of the absence of N-H and C=N bonds and the more rigid structure of pentacene.

Figure 24 gives the very preliminary results obtained with anthracene and shows clearly the evidence for a similar electron-electron excitation. Further results will be required before a definite picture of the effect of anthracene on the TED can be obtained.

SUMMARY

Both phthalocyanine and pentacene greatly alter the TED structure of W and Mo. A study of the temperature, shape and field dependence of the TED curves identify both electron-electron and electron-phonon interactions in the phthalocyanine results. Elastic tunnel resonance cannot be ruled out as a possible mechanism in some of the pentacene results although no electron-phonon interactions were identified. Steric effects undoubtedly account for some of the apparent irreproducibility of the results; however it is not yet clear to what extent steric or partial decomposition effects influence the TED results. It is reasonably certain that structure in the TED of field emitted electrons will be observed in aromatic compounds and that this structure will eventually be interpretable in terms of the electronic and phononic spectra of the adsorbed molecule. To the extent that the molecular patterns represent single molecules, the spectra so observed can be confined to a single adsorbed molecule.

REFERENCES

1. J. Lambe and R. Jaklevic, Phys. Rev. 165, 821 (1968).

2. W. Thompson, Phys. Rev. Letters 20, 1085 (1968).

3. C. Duke and M. Alferieff, J. Chem. Phys. 46, 923 (1967).

4. L. Swanson and L. Crouser, Final Rept., Contract NASw-1516, Nov. 1968.

5. E. Plummer, J. Gadzuk and R. Young, Solid State Comm. 7, 487 (1969).

6. D. Flood, NASA Tech. Note D-5423 (1969).

7. D. Scalapino and S. Marcus, Phys. Rev. Letters 18, 459 (1967).

8. A. Melmed and E. Müller, Tech. Rep. AFOSR-TN58-646 (1958), ASTIA, AD No 162178.

9. A. Ebert and H. Gottlieb, J. Am. Chem. Soc. 74, 2806 (1952).

10. G. Herlmeier and G. Warfield, J. Chem. Phys. 38, 893 (1963).

11. A. Sidorou and I. Kotlyar, Optics and Spectroscopy 11, 92 (1961).

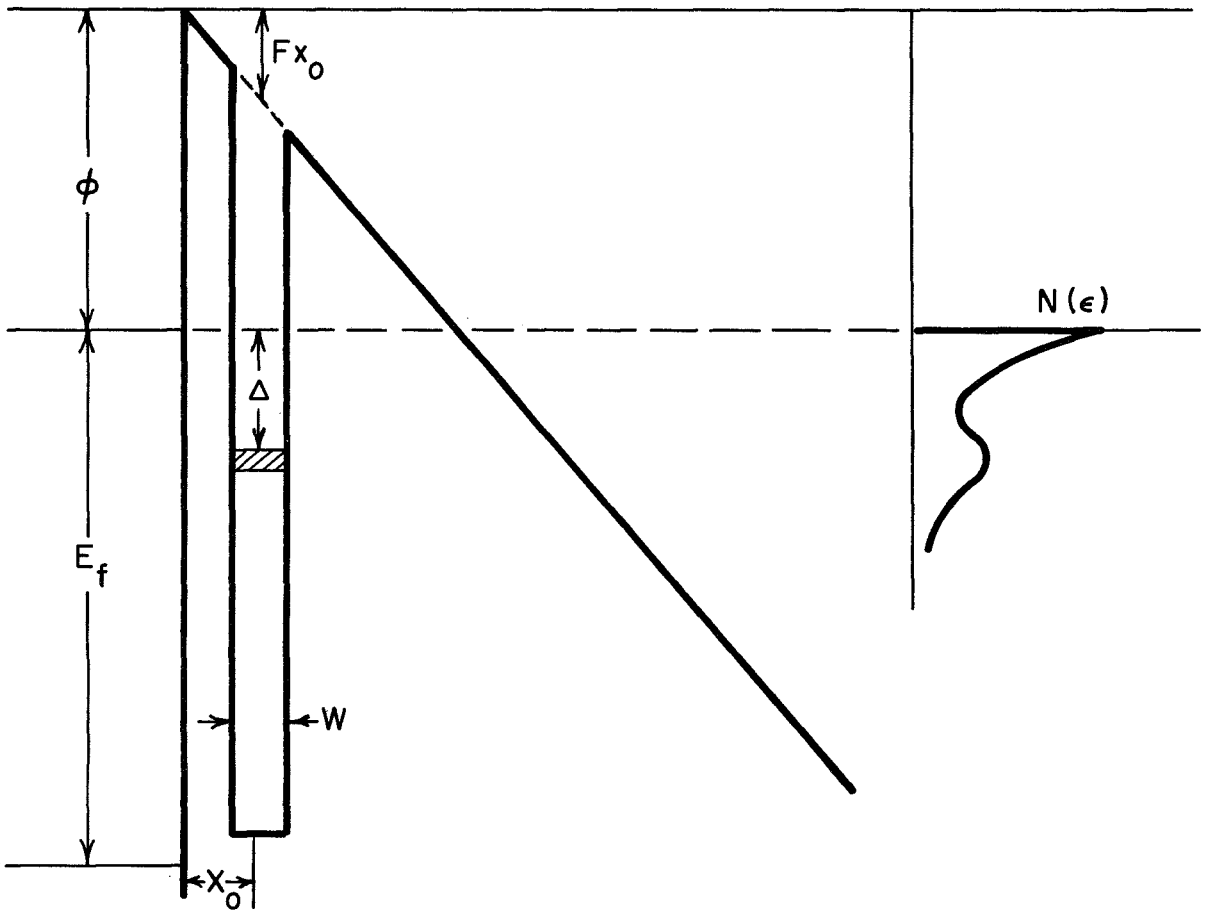

Figure 1 Electric potential energy diagram for tunnel resonance enhanced field emission.

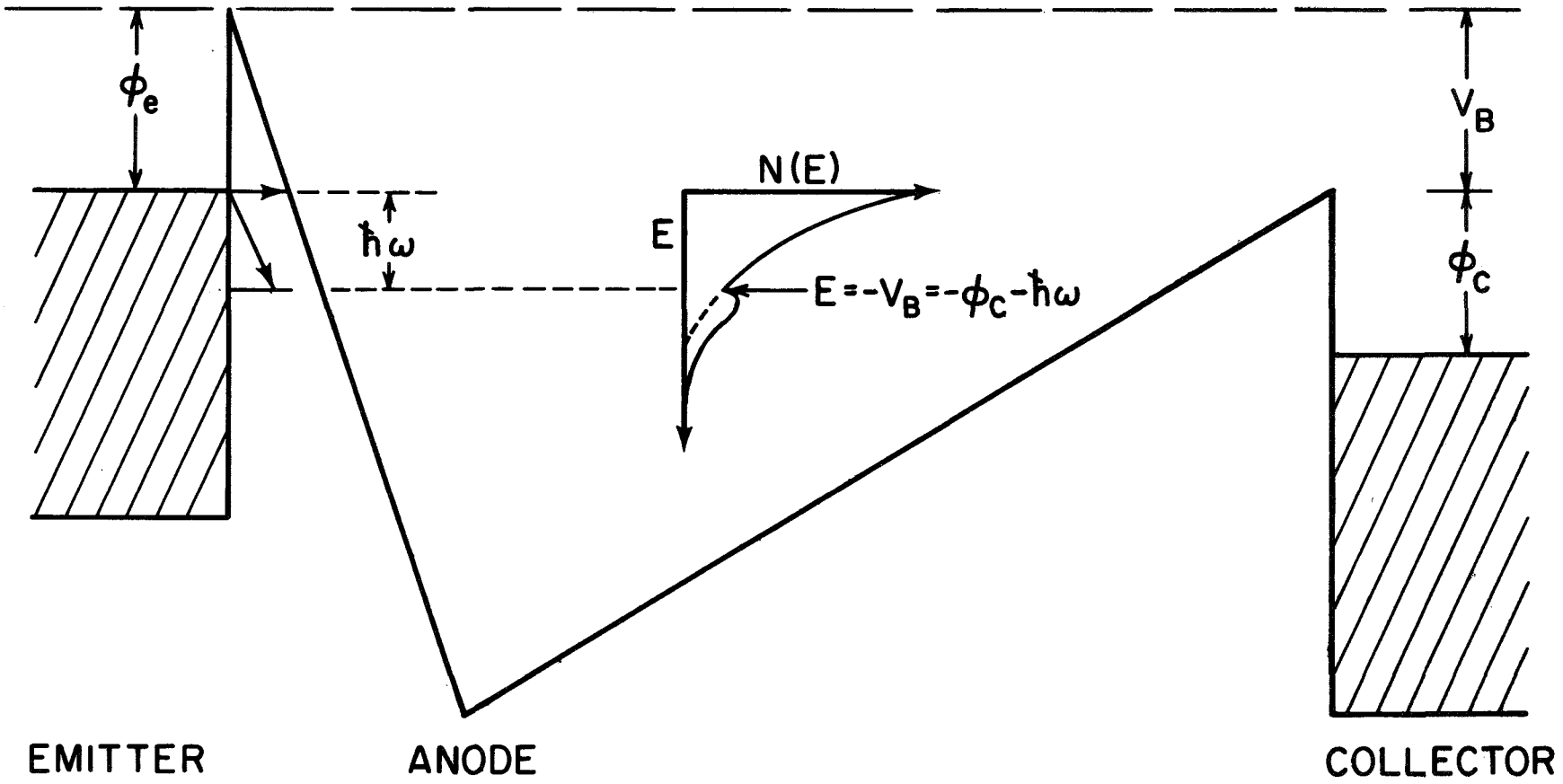

Figure 2 Electric potential energy diagram for electron-phonon interaction during field emission.

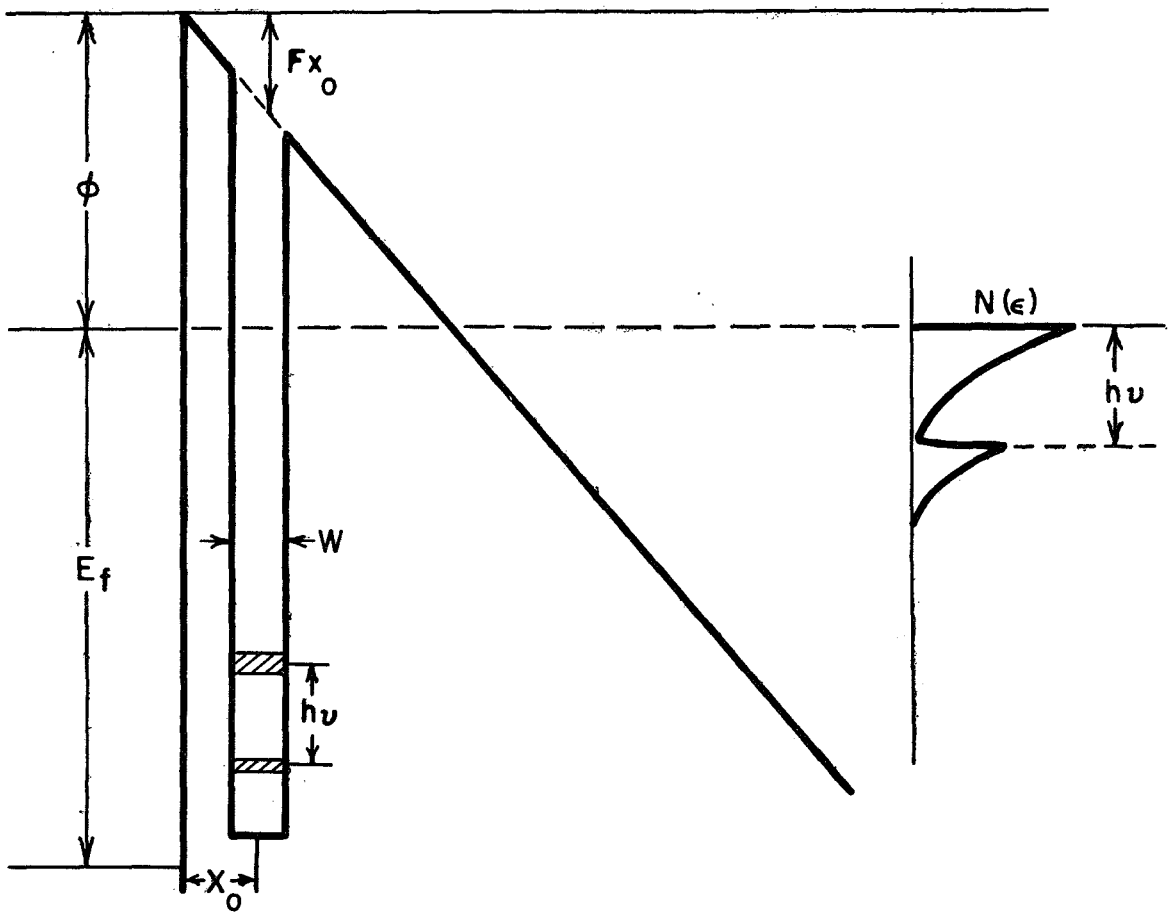

Figure 3 Electric potential energy diagram for electron-electron interaction during field emission.

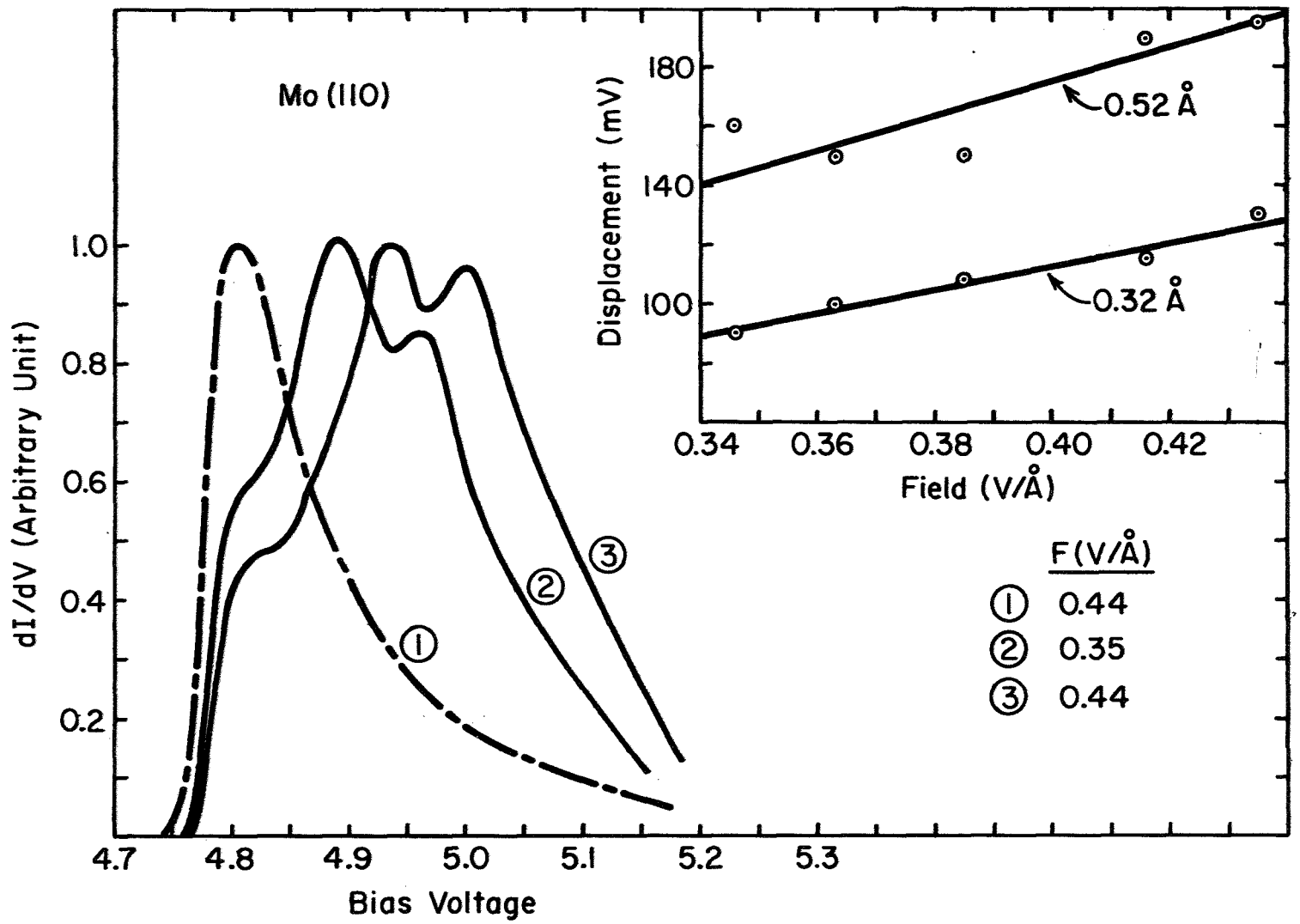

Figure 4 TED spectra for pht. on Mo (110); I_a/I_c = 27; curve 1 is clean TED.

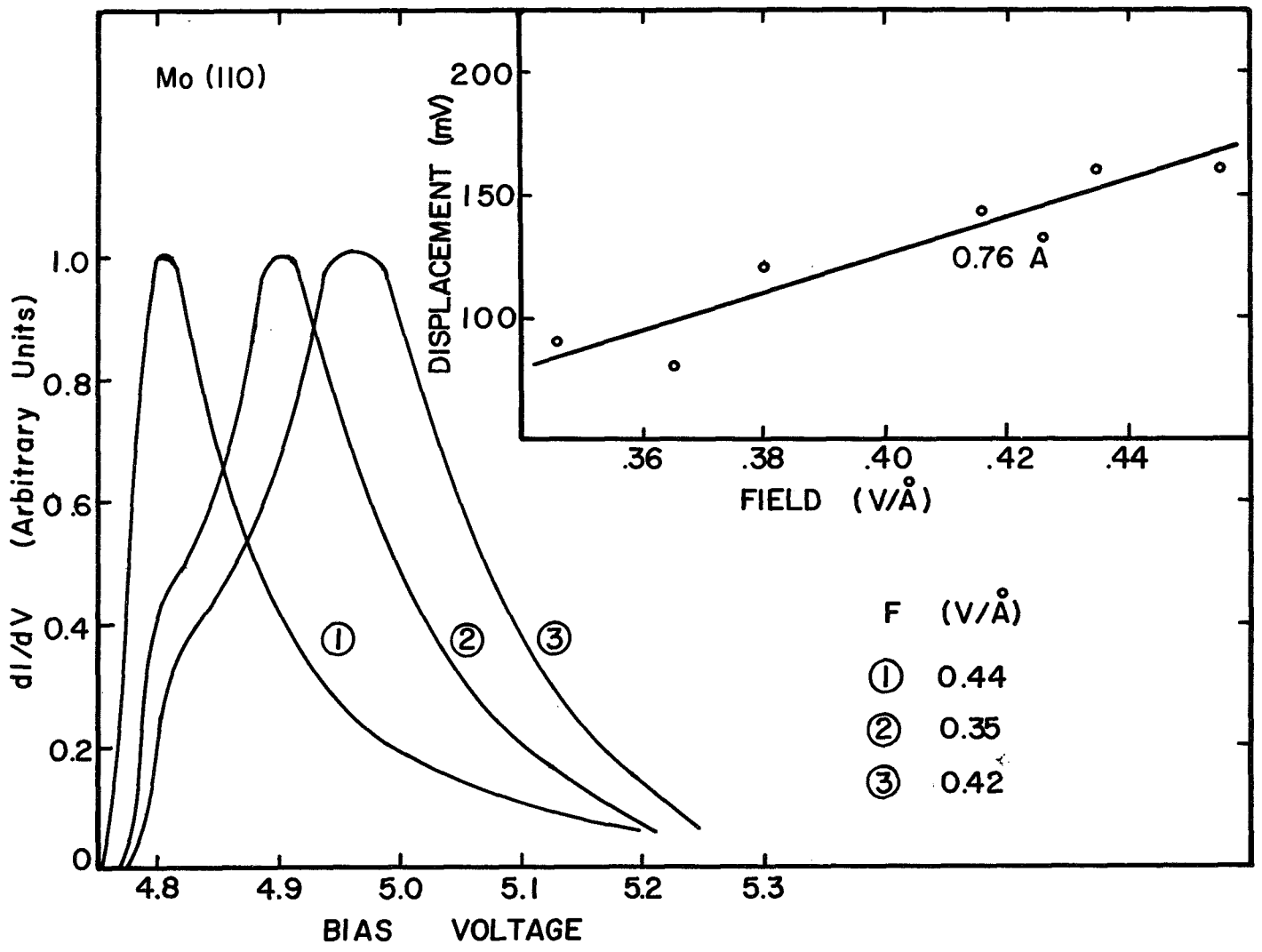

Figure 5 TED spectra for pht. on Mo (110); $I_a/I_c = 3.5$; curve 1 is clean TED.

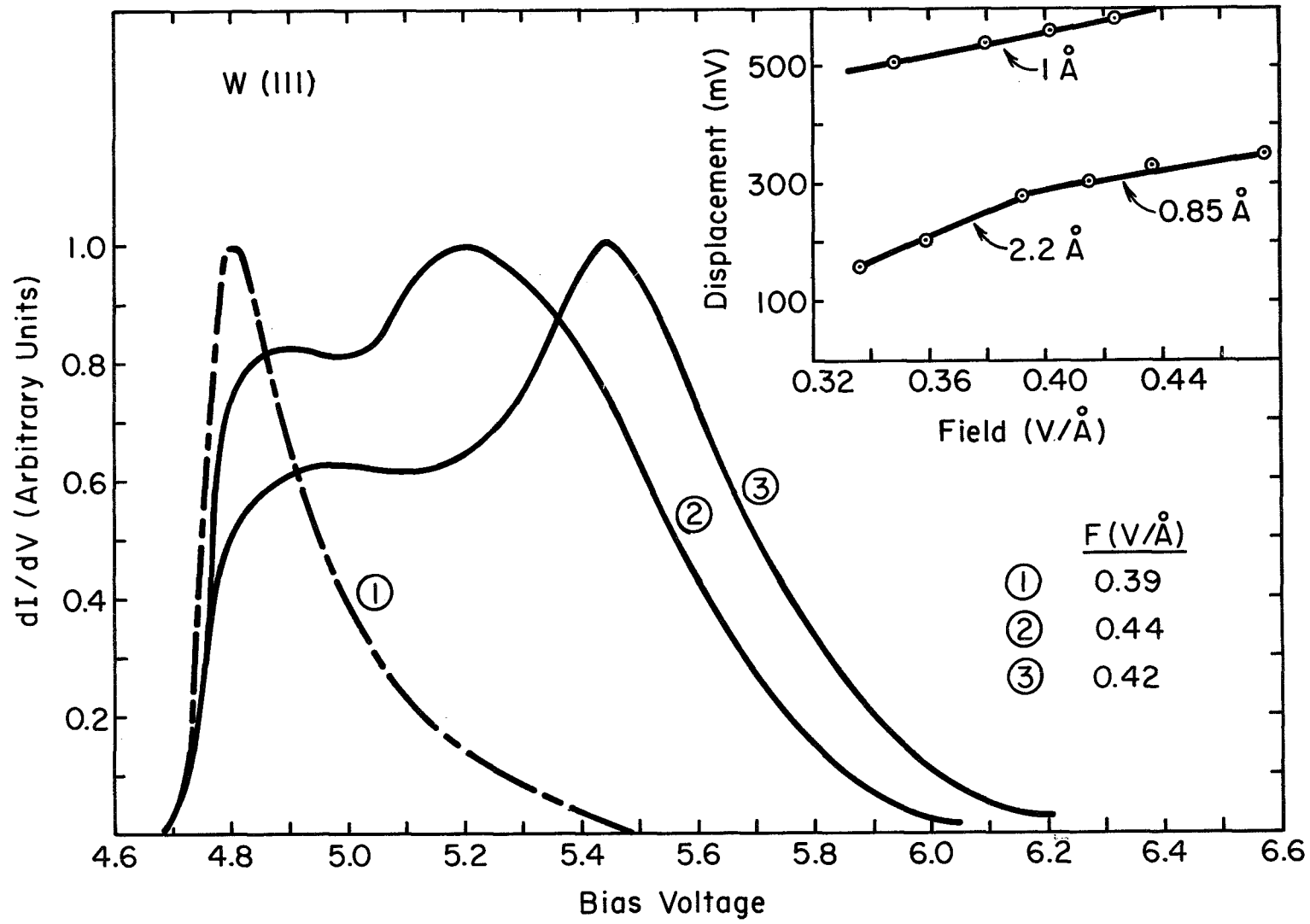

Figure 6 TED spectra for pht. on W (111); curve 1 is clean; curve 2, $\Delta\phi$ = -0.3 eV, B = 0.3, I_a/I_c = 2.7; curve 3, $\Delta\phi$ = -0.9 eV, B = -2.0, I_a/I_c = 4.2. Curves 2 and 3 represent two different depositions.

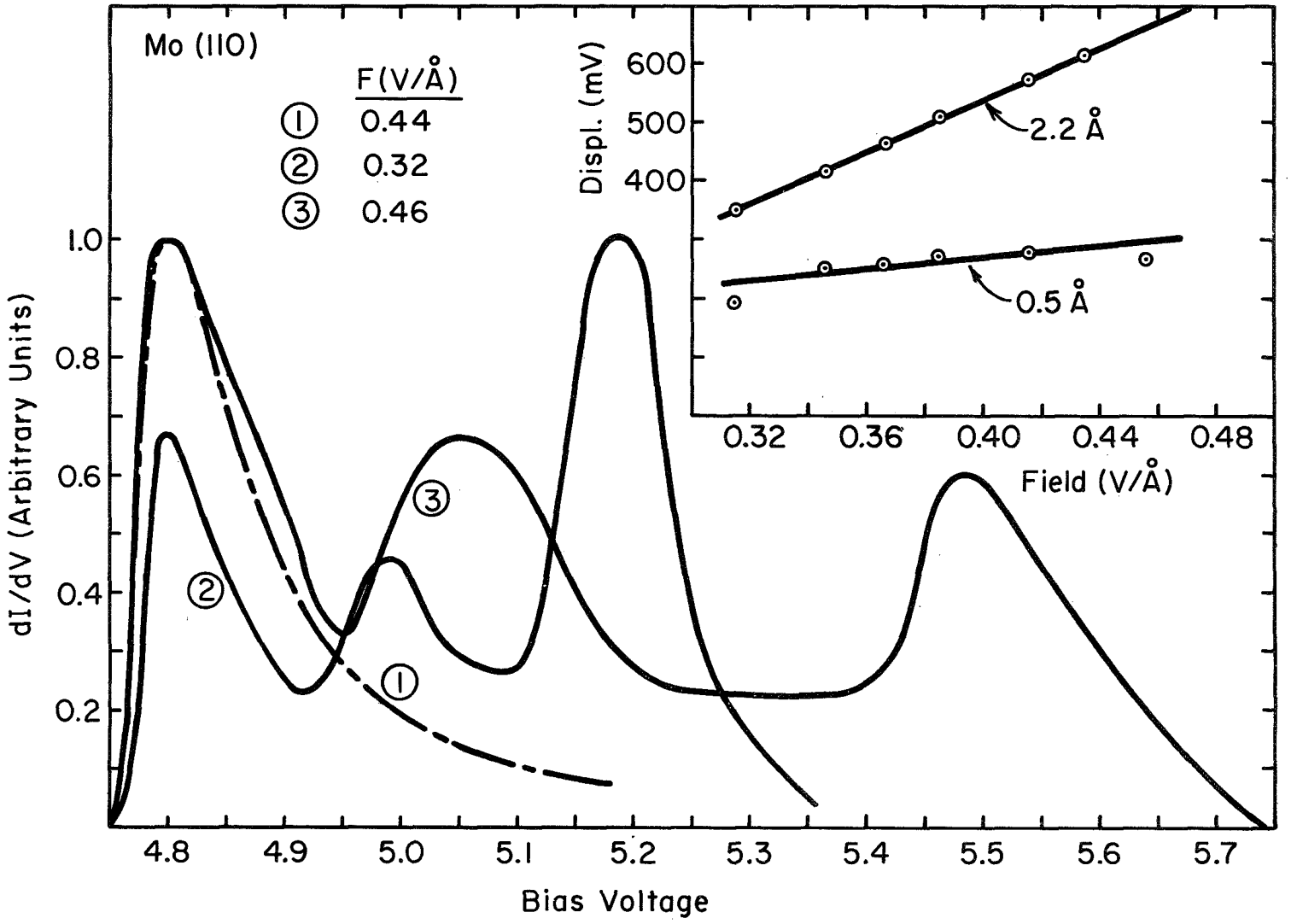

Figure 7 TED spectra for pht. on Mo (110); curve 1 is clean; $\Delta\phi$ = -0.48 eV; B = 0.4; I_a/I_c = 170.

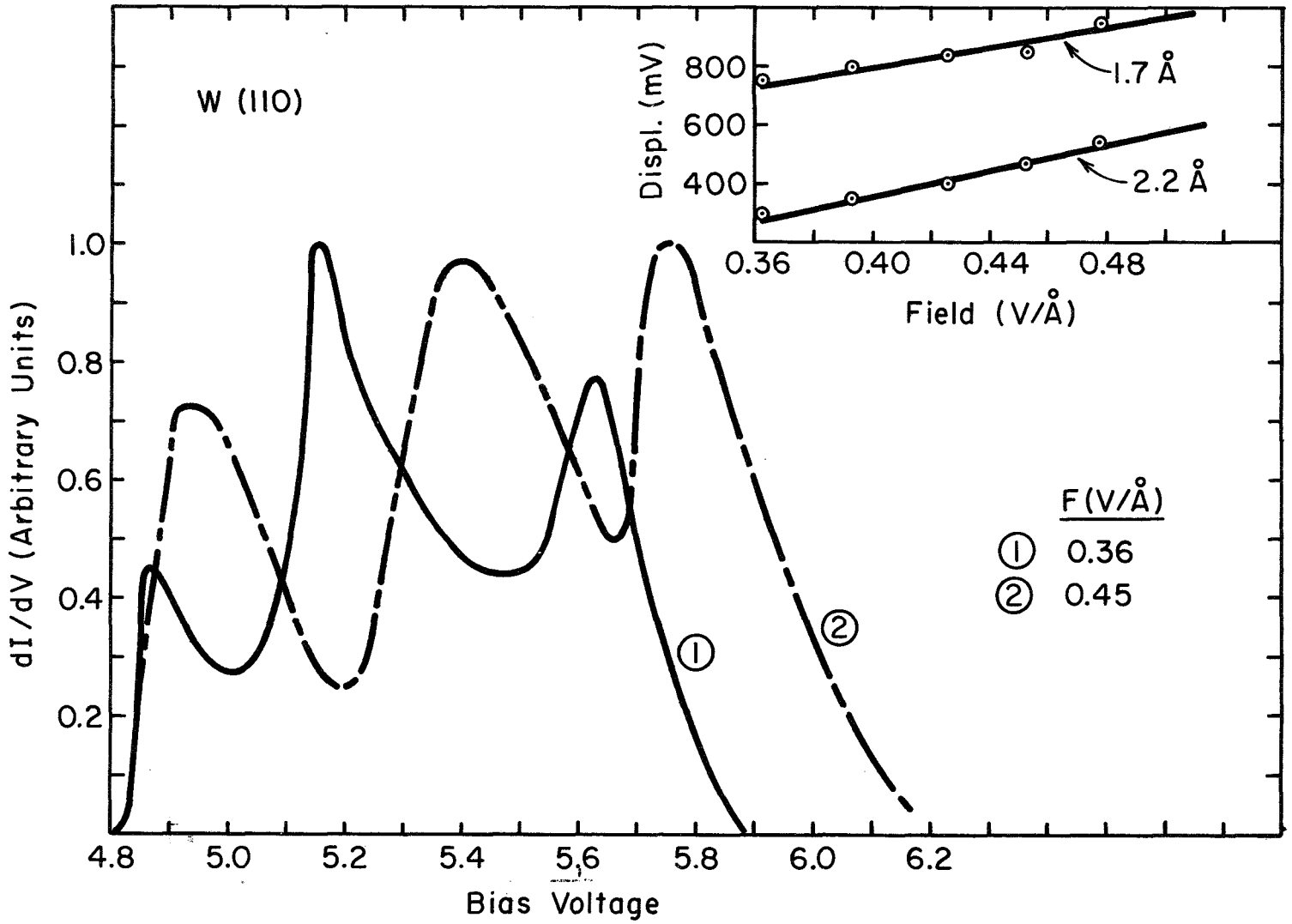

Figure 8 TED spectra for pht. on W (110); $\Delta\phi$ = 0. 62 eV; B = -0. 3; I_a/I_c = 25.

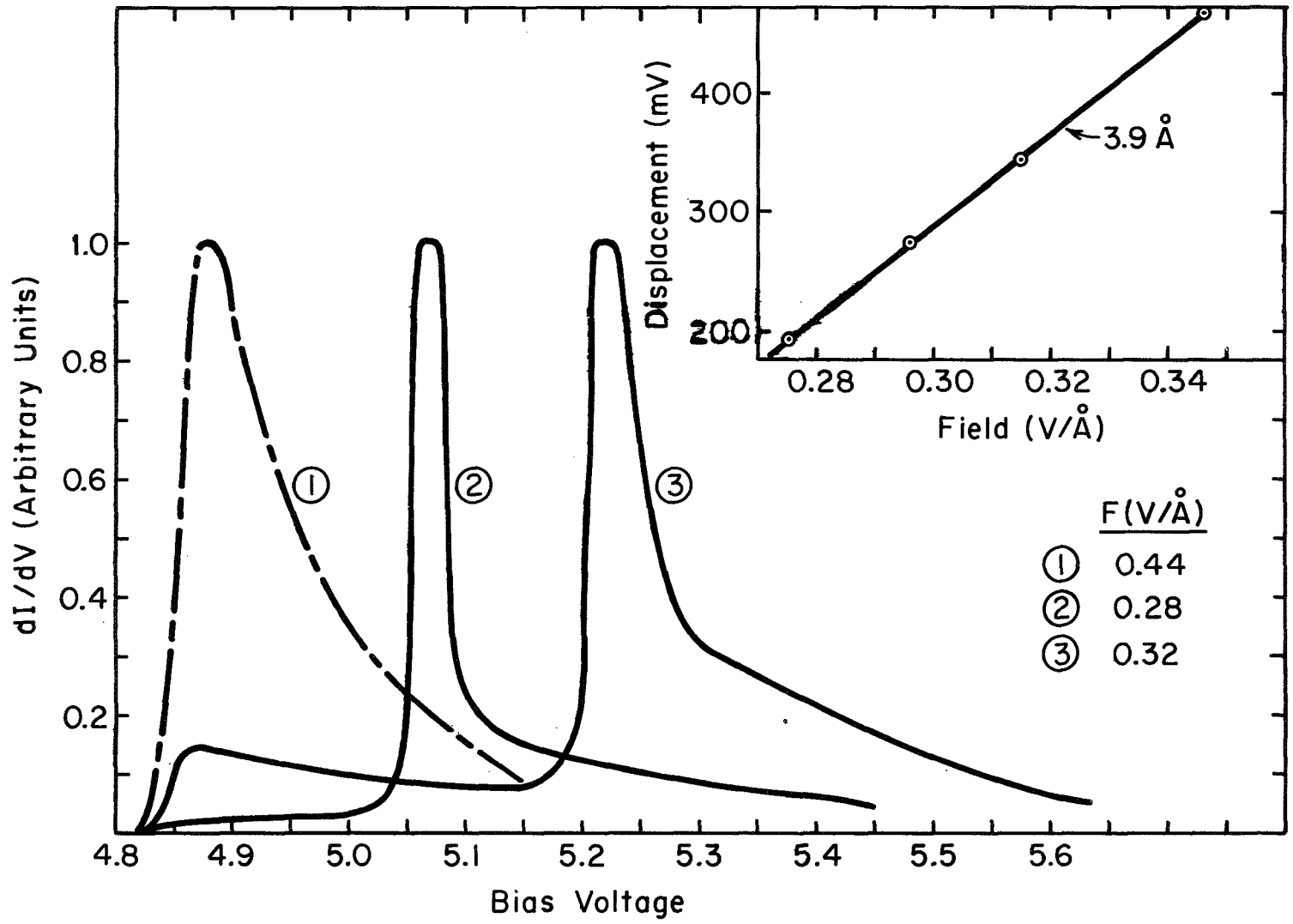

Figure 9 TED spectra for pht. on Mo (110); curve 1 is clean; $\Delta\phi$ = -1.0 eV; B = 1.0; I_a/I_c = 880.

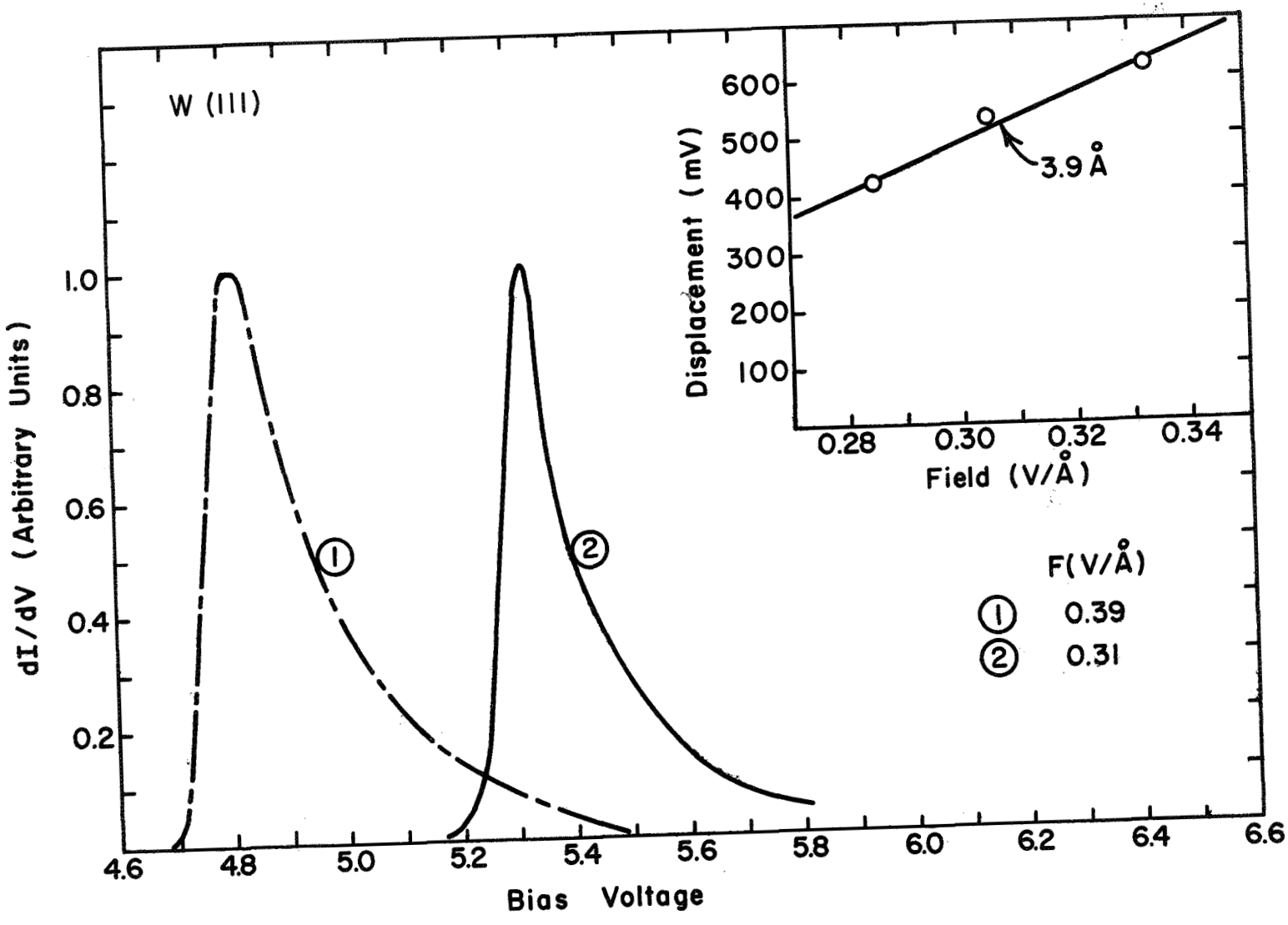

Figure 10 TED spectra for pht. on W (111); curve 1 is clean.

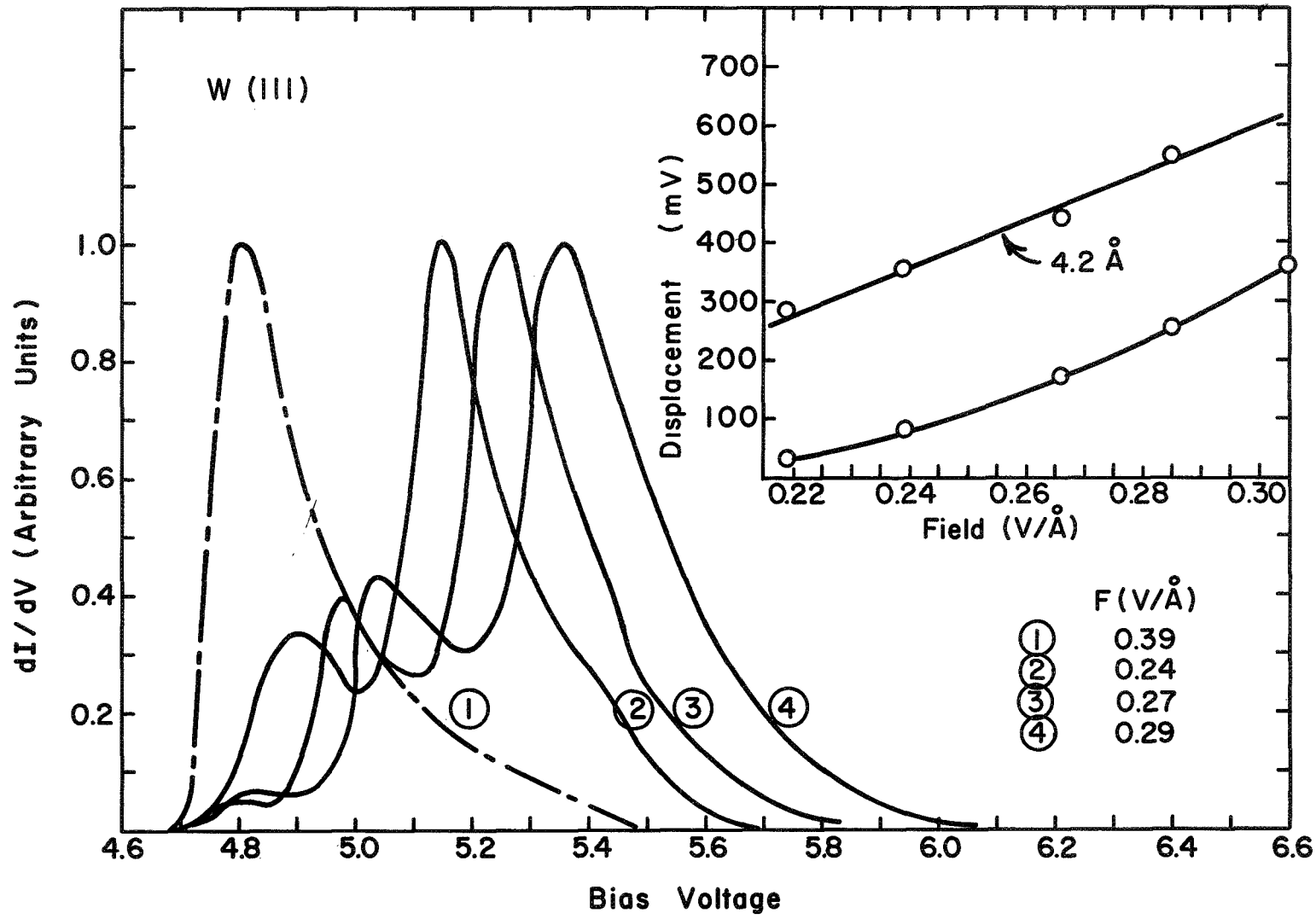

Figure 11 TED spectra for pht. on W (111); curve 1 is clean; $\Delta\phi$ = -1.3 eV, B = -0.8; I_a/I_c = 170

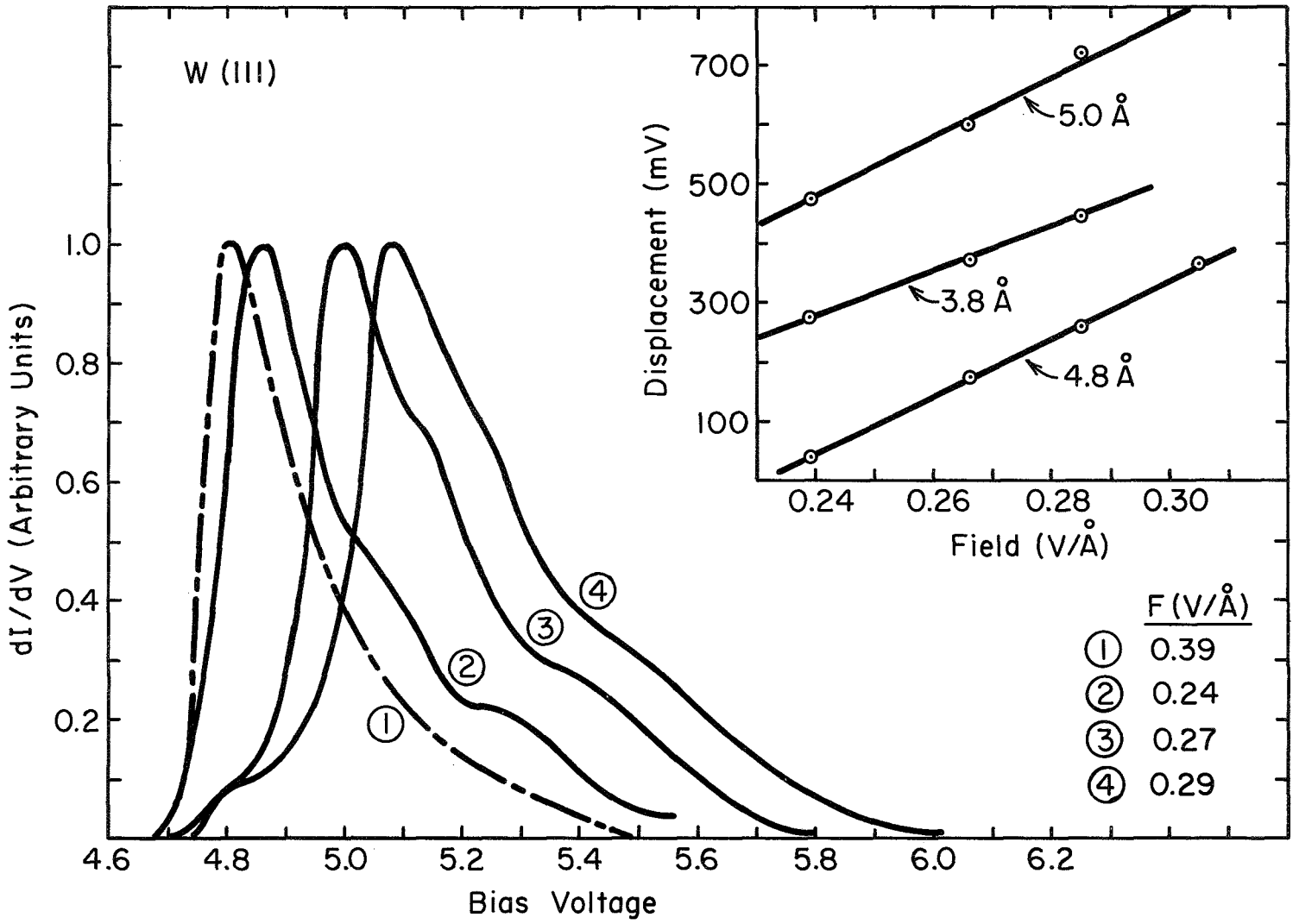

Figure 12 TED spectra for pht. on W (111); curve 1 is clean.

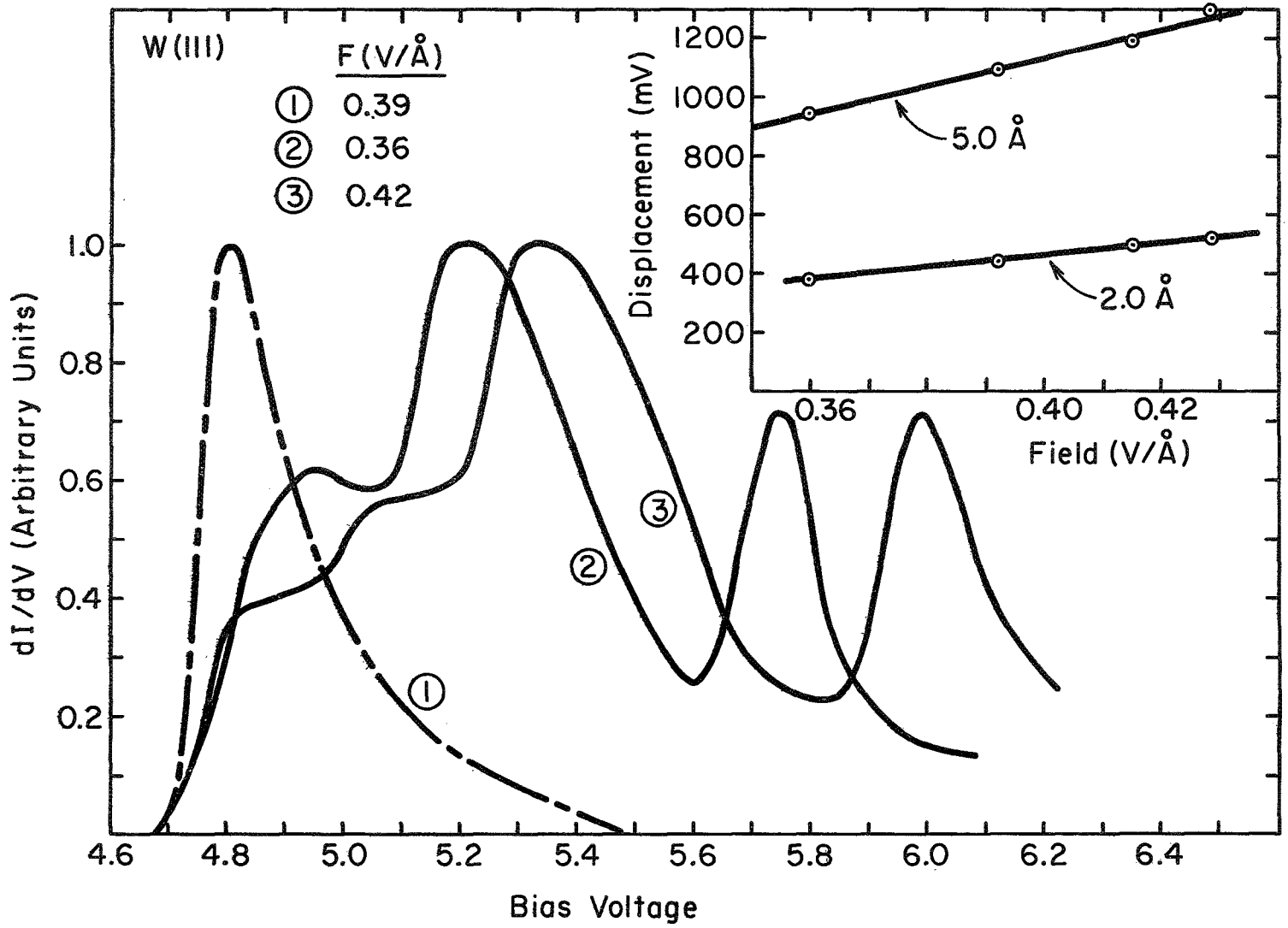

Figure 13 TED spectra for pht. on W (111); curve 1 is clean; $\Delta\phi$ = 0.83 eV; B = -1.0; I_a/I_c = 12.7.

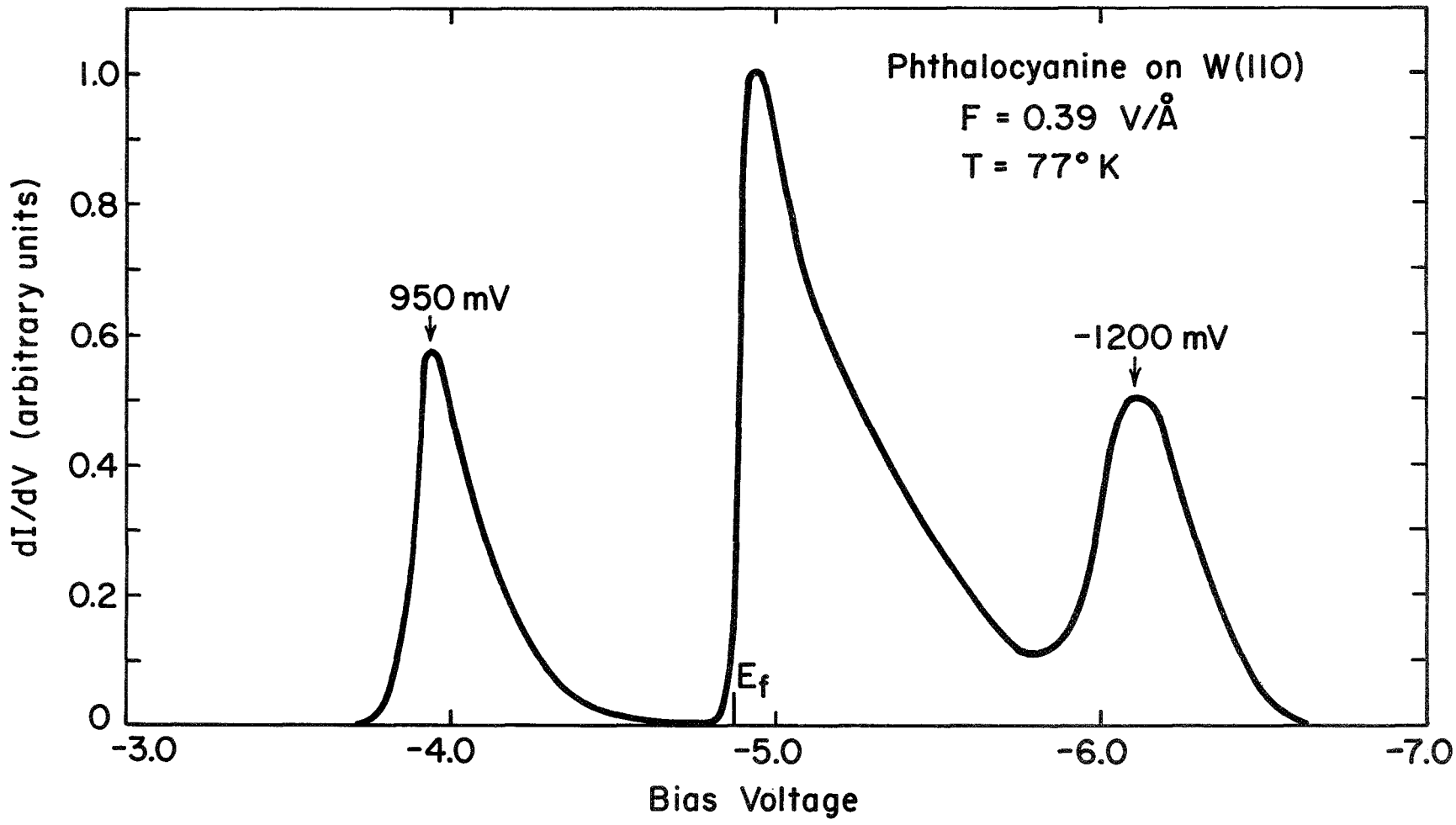

Figure 14 TED spectra pht. on W (110); I_a/I_c = 540. Note the peak 950 mV above the fermi level.

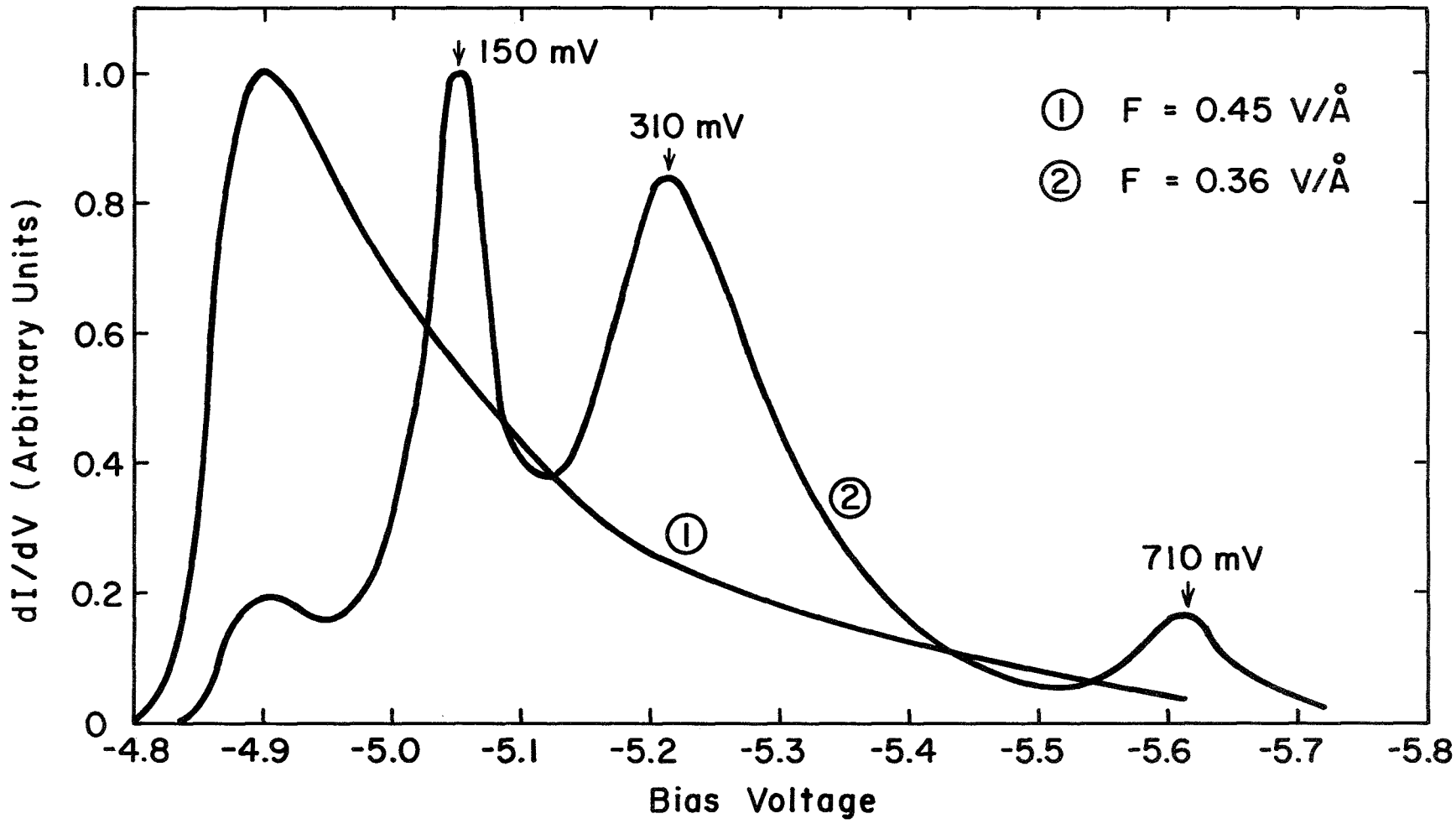

Figure 15 TED spectra pht. on W (110); I_a/I_c = 55. Note three distinct peaks.

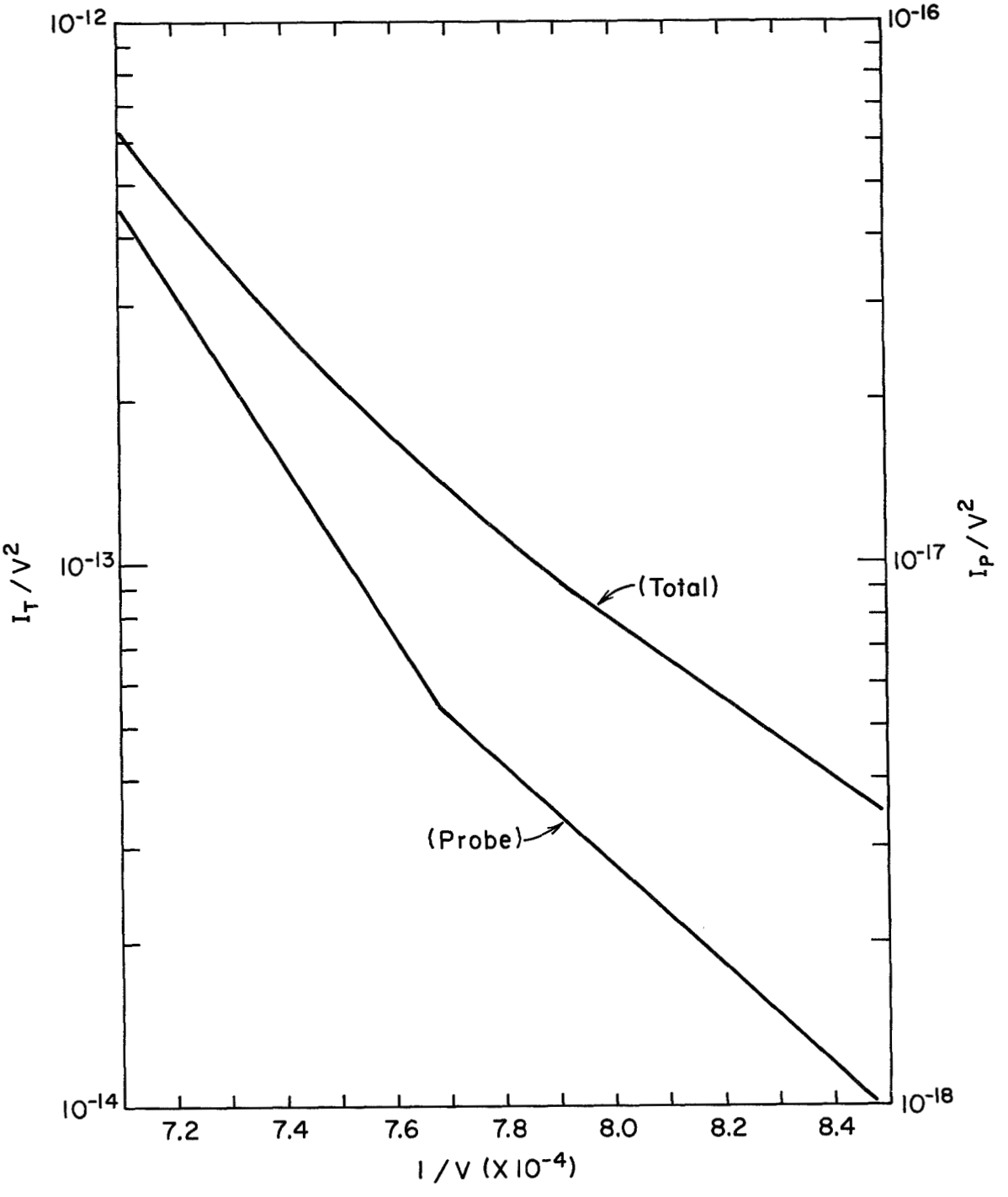

Figure 16 Fowler-Nordheim plot of probe and total current obtained from the TED corresponding to the Figure 15.

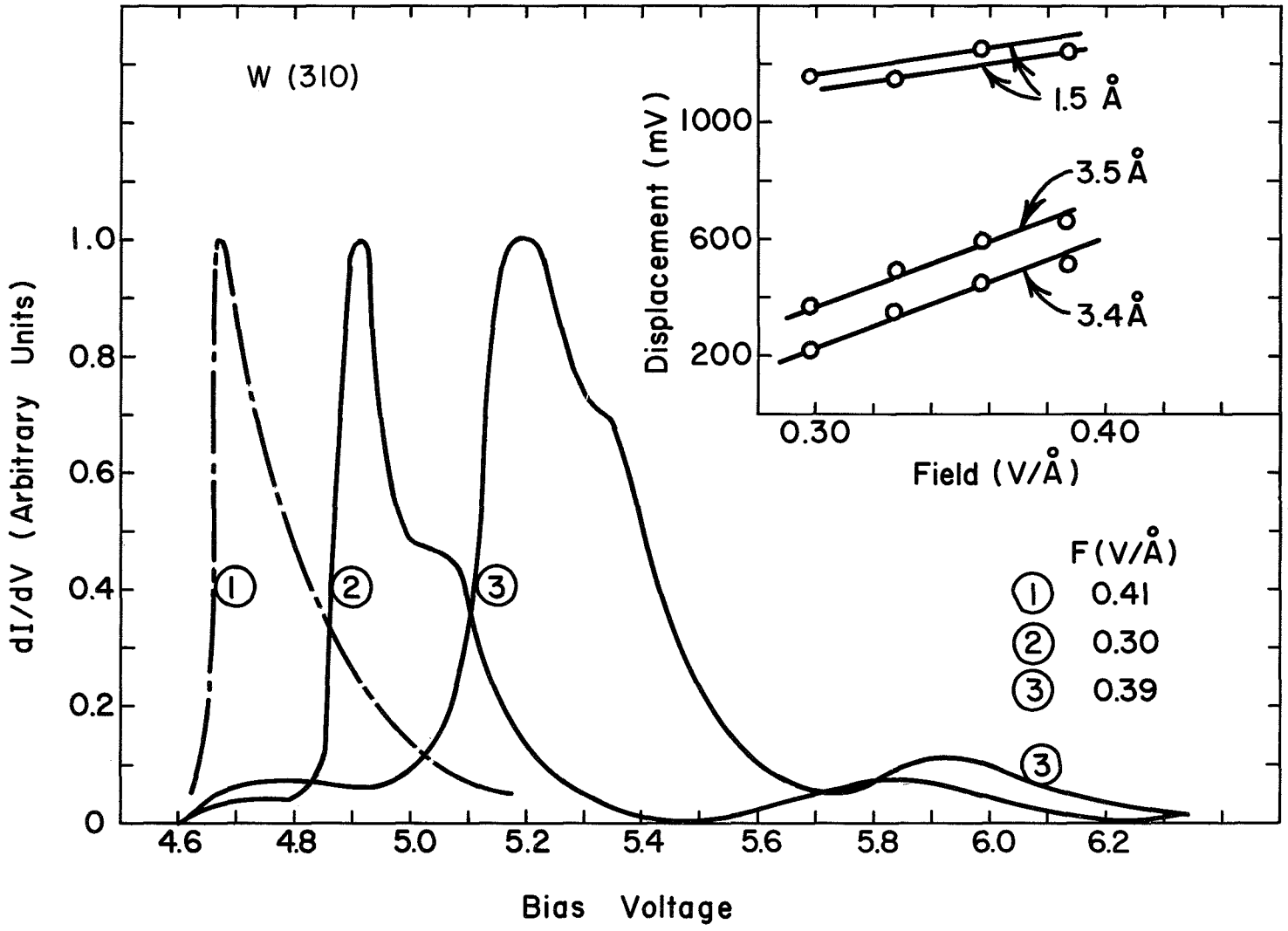

Figure 17 TED spectra pentacene on W (310); curve 1 is clean, $\Delta\phi$ = -1.7 eV, B = 2.0; I_a/I_c = 680.

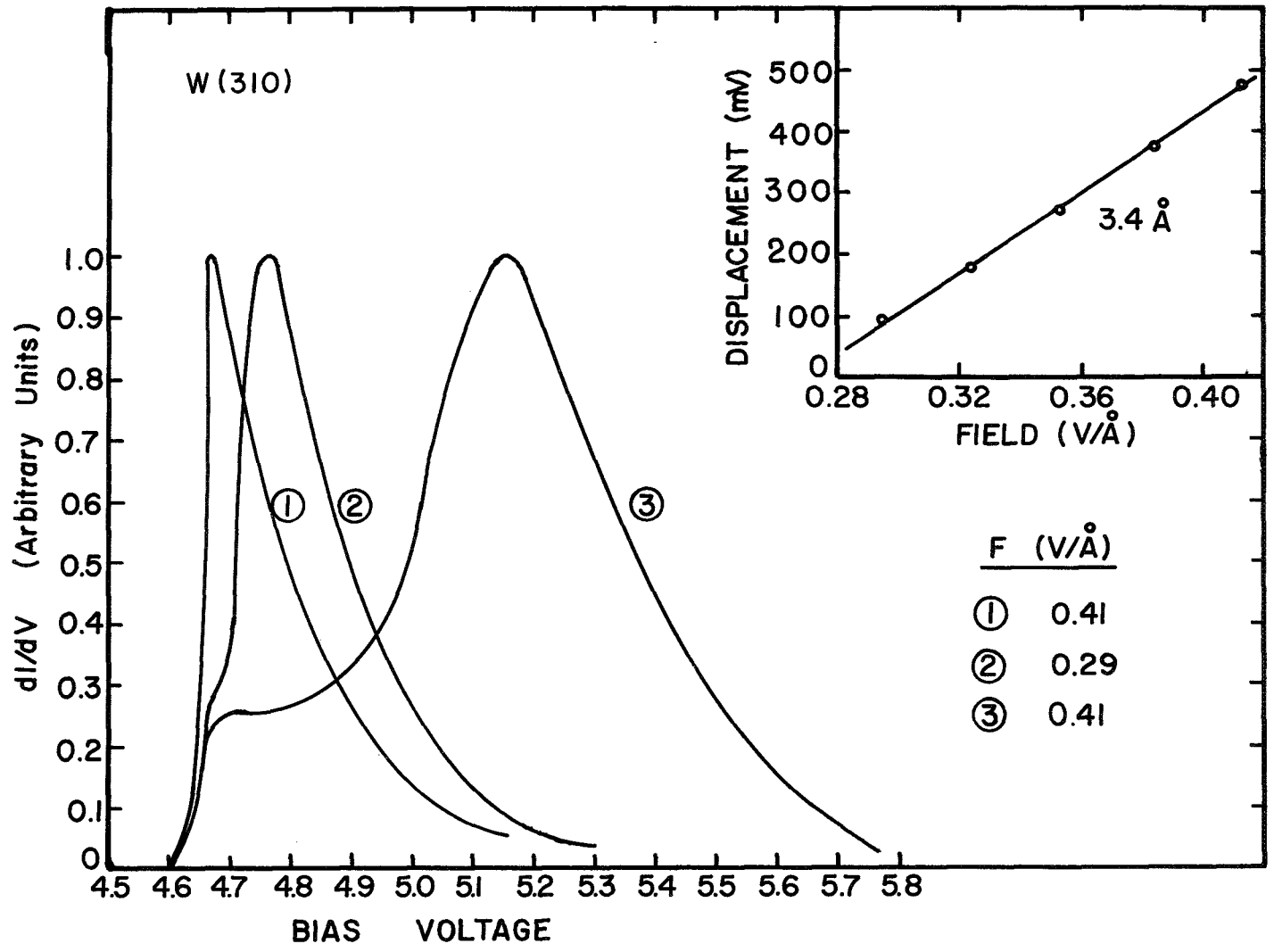

Figure 18 TED spectra pentacene on W (310); curve 1 is clean; $I_a/I_c = 55$.

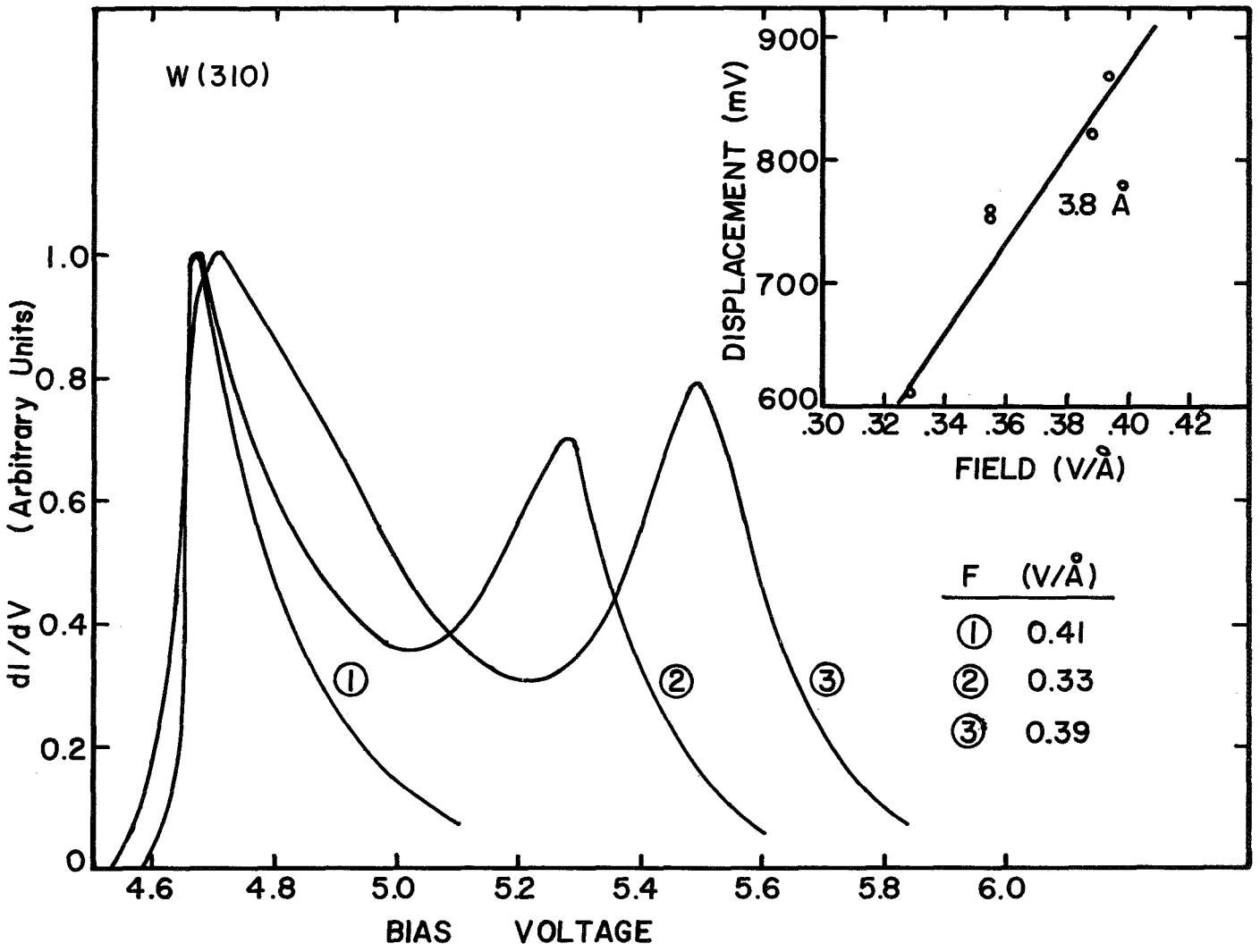

Figure 19 TED spectra pentacene on W (310); curve 1 is clean; I_a/I_c = 2.1.

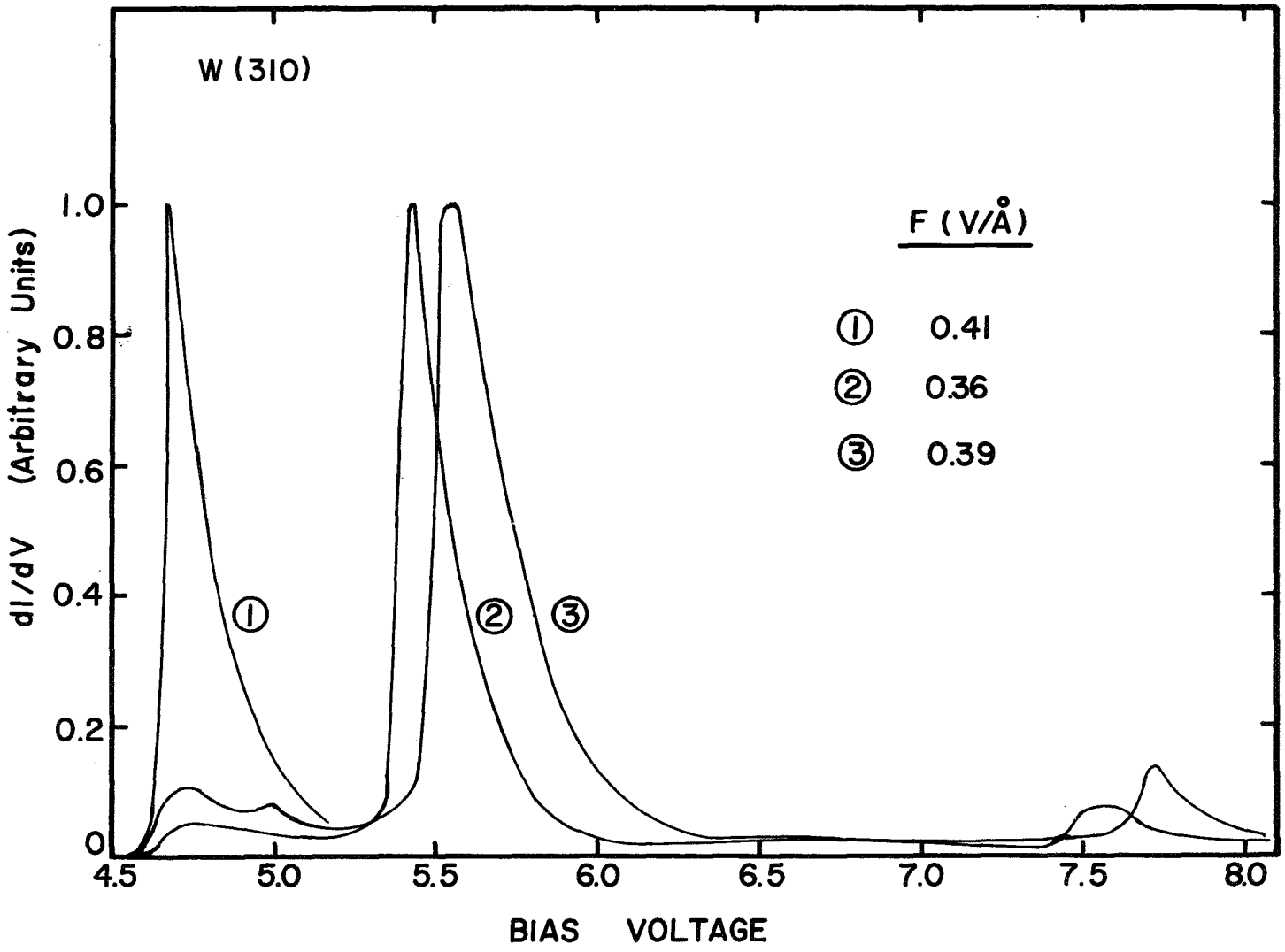

Figure 20 TED spectra pentacene on W (310); curve 1 is clean.

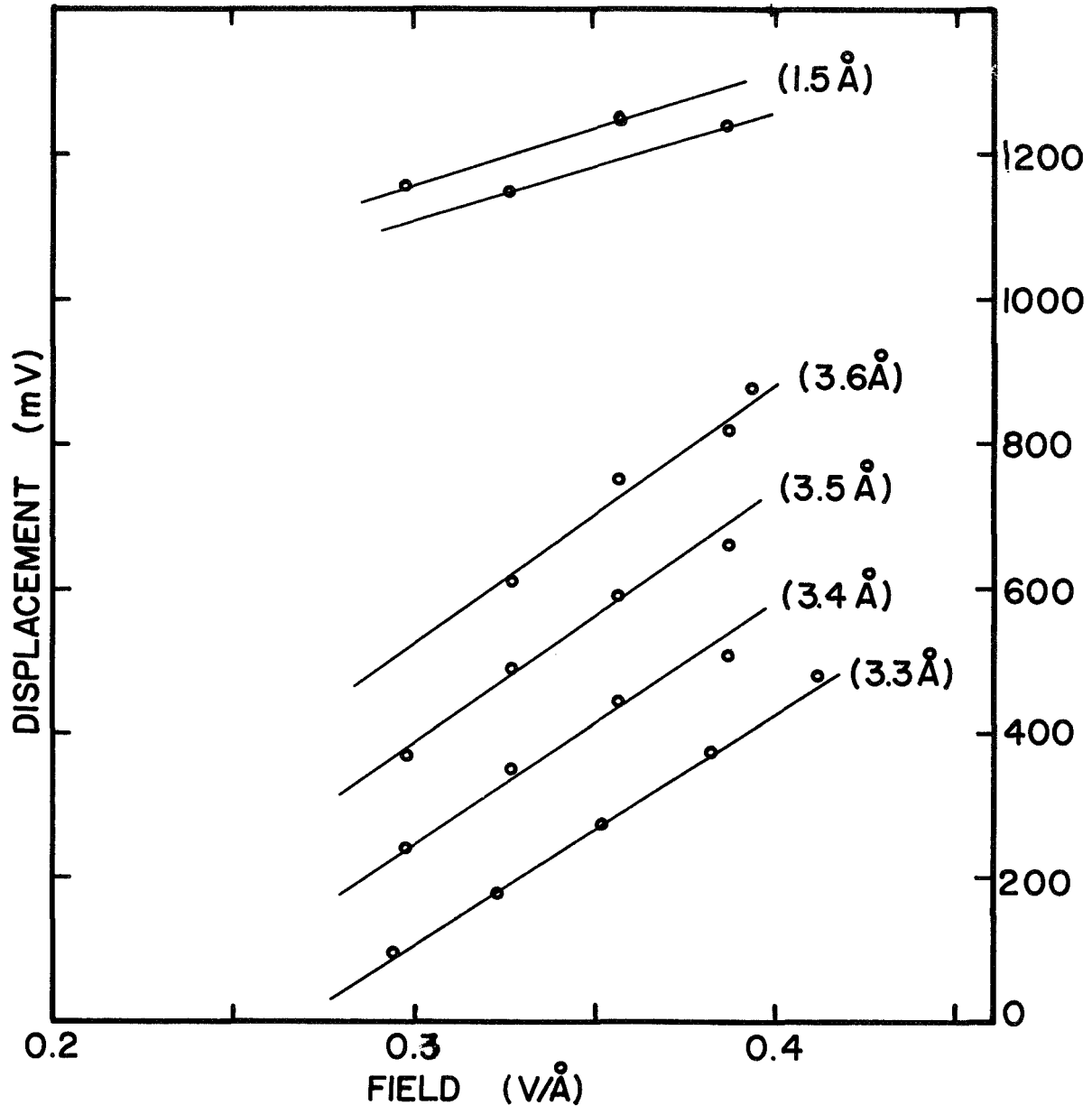

Figure 21 Summary of peak displacements vs field strength for pentacene on W (310).

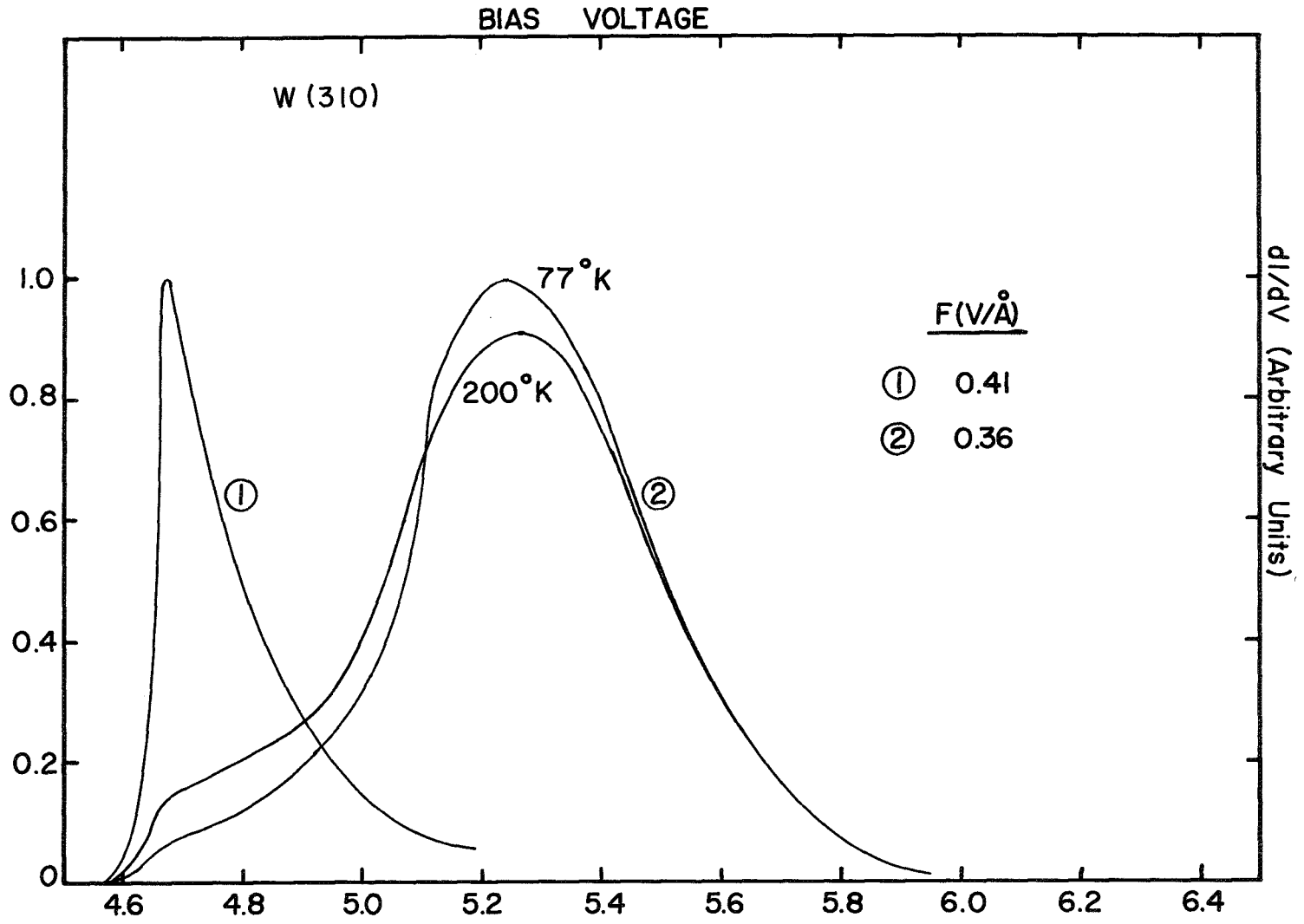

Figure 22 TED spectra pentacene on W (310); curve 1 is clean; $\Delta\phi$ = -0.65 eV; B = -0.6; I_a/I_c = 5.7. The TED is shown at 77 and 200°K.

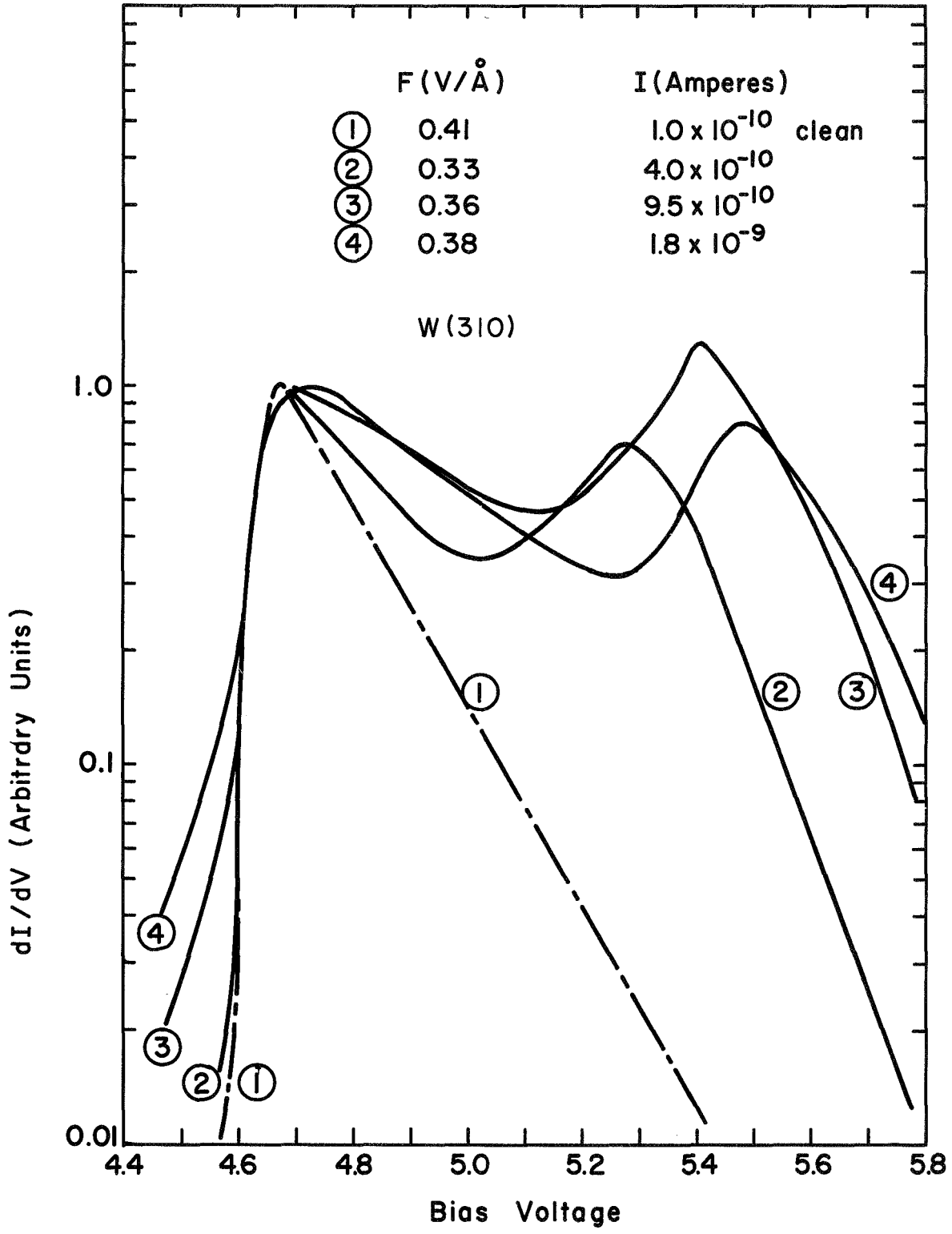

Figure 23 Replot of TED in Figure 19; Note change in leading edge as a function of field (or current).

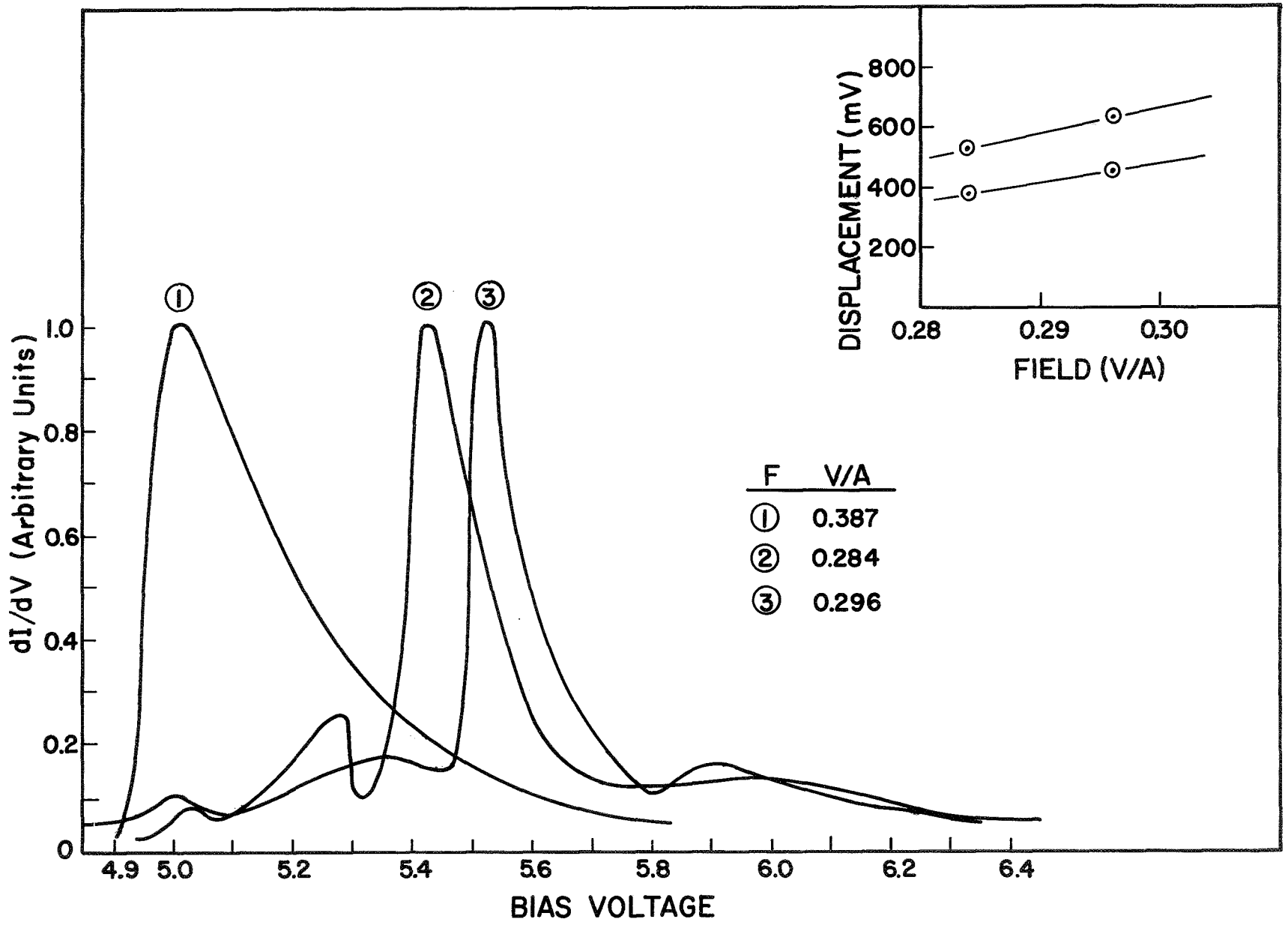

Figure 24 Energy distribution of Anthracene adsorbed on Tungsten (310) emitter.

II. Investigation of the Total Energy Distribution of Field Emitted Electrons From Rhenium

INTRODUCTION

The first section of this report deals entirely with the effects of adsorbed molecules on the total energy distribution (TED) of field emitted electrons. It has been indicated in previous reports that band structure effects may under certain circumstances alter the TED obtained from clean metal surfaces.[1] Recent theoretical and experimental investigations have prompted us to devote a portion of this study to further investigation of the TED from clean metals with emphasis being placed on those metals whose band structure might alter the TED from that predicted by Fowler-Nordheim (FN) field emission theory. Such effects have been observed and were reported for both tungsten and molybdenum.[2] In addition recent studies[3] show a similar result along the <111>direction of copper which contains the neck of an otherwise spherical Fermi surface. According to calculations, other metals that may exhibit band structure effects on the TED are N <111> and possibly Re<0001>. Another important criterion which must be taken into account is the difficulty in fabricating field emission cathodes and the practicality of cleaning after fabrication. For this reason and because of its availability and familiarity we have selected rhenium.

The theory of field electron tunneling from metal into vacuum has been developed for some time. Recent work directed towards the inclusion of band structure considerations has appeared in the literature and examines

several different but probably related effects. Stratton[4] has derived theoretical expressions for the TED from metals with arbitrary Fermi shape but with $E \propto \bar{k}^2$. Itskovitch[5] investigated the influence of Bragg reflections and considered the effects of an open Fermi surface on the TED. An open Fermi surface along the emission direction should result in a shift of the peak in the TED curve toward the bottom of the conduction band. This can be explained by noting that an open Fermi surface along a particular direction means no electrons at the Fermi energy possess momentum vectors along the emission direction. Depending on the angular size of the Fermi surface opening, the TED peak will shift toward the Fermi level as one measures the TED at increasing angles from the direction of the open Fermi surface.

Both Stratton and Itskovitch have considered the effect of arbitrary Fermi shapes on field emission TED but where the energy (E) retains a parabolic relationship with respect to momentum space ($\bar{k}$), as found in free electron like bands. Gadzuk[6] has attempted to explain band structure effects on tunneling by avoiding the assumption of a parabolic E-k relationship and considered an approximate band shape by superposition of a free s-like band and a tight binding d band. His purpose was to demonstrate that the density of states and non-parabolic bands can be as important as Fermiology considerations in determining the TED.

Recent calculations by Mattheiss have yielded a theoretical model for the Fermi surface of rhenium which shows some interesting band structure near the Fermi level.[7] The electronic $E(\bar{k})$ relationships calculated by

Mattheiss for rhenium are shown in Figs. 1 and 2. Fig. 1 shows the relativistic energy bands for rhenium neglecting spin-orbit coupling and Fig. 2 shows the effects of spin-orbit coupling. The individual bands are not labeled in the case of spin-orbit coupling since the calculations were carried out using unsymmetrized basis functions so it was not possible to label the symmetry properties of the individual state.[7]

EXPERIMENTAL

TED measurements were made in a van Oostrum type analyzer of the type previously reported.[1] For part of the experiment the tube was altered by exchanging the dipole magnet with a four segment (quadrupole) anode so that deflection could be accomplished by the more convenient electrostatic method.

Two crystal orientations have been examined. First a rhenium emitter oriented approximately in the $\langle 10\bar{1}0 \rangle$ direction was examined in the magnetic type deflection tube. Next a $\langle 0001 \rangle$ oriented emitter was examined in the electrostatic deflection quadrupole tube. The resolution obtained from the first tube as estimated from the TED curves was less than 40 mV at 77°K. The second tube gave a resolution of about 80 mV at 77°K. These resolution values were obtained using the criteria introduced by Young and Kuyatt of measuring the energy difference between the 10 and 90% points on the TED leading edge.[8]

RESULTS

Since magnetoresistance experiments have exhibited fairly conclusive evidence of an open orbit in the Fermi surface along the <0001> direction of Re[9, 10], the most obvious deviations which might be expected to occur in the TED curve from <0001> Re would be an energy shift in the onset of emission as predicted by Itskovitch[5] and observed by Whitcutt and Blott from the <111> direction of copper.[3] Fig. 3 shows the calculated intersections of the Fermi surface with the symmetry planes of the Brillouin zone. Fig. 4 shows the Brillouin zone for the hexagonal crystal structure.

The data obtained from the <0001> direction is shown in Fig. 5. No shift was observed in the onset of emission as the beam was deflected from the <0001> direction towards the lower work function areas as shown by the second curve in Fig. 5. The value of absolute work function (ϕ_e) determined from the slope of the TED and FN plots was 5.8 eV.[1] A determination of work function (ϕ_f) from FN plots gave a much larger value of 6.5 eV, by assuming a value of 4.88 eV for the average work function and assuming that the value of the field factor (β) for the (0001) plane was the same as the average. No obvious structure was detected in the TED for the (0001) plane of rhenium over a range of about 0.5 eV below the Fermi level, which is the limit of detectability.

The TED obtained from the $<10\bar{1}0>$ direction is shown in Fig. 6. Note the hump present on the distribution that extends from about 0.3 eV to about 0.4 eV below the Fermi level. By ignoring the presence of the hump, the

value of the absolute work function (ϕ_e) calculated from this plane was 4.1 eV.

DISCUSSION

This preliminary data obtained from rhenium indicated an anomalous behavior of the electron emission from the $<10\bar{1}0>$ and possibly the $<0001>$ directions. Such behavior, not predicted by classical FN field emission theory, suggests that the band structure of rhenium may influence the electron emission from these planes.

Since magnetoresistance experiments,[9,10] show a large open surface along the Γ A (or 0001) direction for rhenium, one might expect a TED similar to that obtained by Whittcutt and Biott from the $<111>$ direction of copper.[3] Such an effect, however, was not experimentally observed and closer examination of the calculated band structure of rhenium indicates that it may not be expected. The band structure along the Γ A direction as shown in Fig. 1 has a band labeled Δ_2 cutting through the Fermi level and extending downward for about 10 eV. This band remains nearly unchanged when spin-orbit coupling is considered in Fig. 2. This band is assumed by Mattheiss to be a 6p-type state. In the case of copper, no similarly positioned band is calculated and there appears to be a total band gap in the region near the Fermi level.[11,12] There is some question as to the actual position of the Δ_2 band since de Has-van Alphen (dHvA) studies give no indication that this band lies above the rhenium Fermi level.[13,14] The calculations which show this band passing through the Fermi level account for the small ellipsoidal hole pocket surrounding Γ as shown in Fig. 3.[7] Since this piece is a

closed surface, it should have been observed in the dHvA data. Our field emission results suggest that the Δ_2 electron band does in fact cross the Fermi level along Γ A and thereby accounts for the existence of the small hole surface at Γ.

No structure within 0.5 eV of the Fermi level was experimentally detected in the TED obtained from the <0001> direction of rhenium and the overall shape of the curve agrees with classical FN theory. However, as pointed out earlier, when an attempt was made to calculate the work function of this plane it was found that the absolute work function (ϕ_e) determination and the FN method (ϕ_f) gave far different results. This indicates possible violation of the internal self consistency of the FN theory along the <0001> direction of rhenium. Calculations indicate that both W <110> and Re <0001> have small hole pockets in these respective directions. The size of the pockets appear to be about the same, that of rhenium being slightly smaller if the band structure calculations are accurate. It is also of interest to note that molybdenum exhibits the same type of hole pocket centered around point N of reciprocal lattice space, but in this case a much larger surface is calculated. Any effect of the hole pockets on the TED from these directions can only be surmised at this time but should be considered as a possible cause for the observed inconsistencies in the FN analysis.

Another possible explanation for the 0.7 eV difference between ϕ_f and ϕ_e for <0001> Re is the variation of the field factor (β) relative to the crystal direction due to local faceting of crystal faces caused by surface energy anisotropy. Müller[15] has found variations of β to be the order of

3% for tungsten (110); thus a variation of 7% for rhenium seems very large indeed, although it should not be considered impossible. The value of ϕ_e (5.8 eV) is only slightly larger than the value determined by thermionic methods (5.6 eV) and may indicate that the local value of β decreases by as much as 7% from the average.

The other plane examined which appears to be rich in band structure near the Fermi level is the $<10\bar{1}0>$ An examination of the energy band for rhenium in the ΓM direction of Fig. 1 shows three states Σ_2, Σ_3 and Σ_4 crossing near the Fermi level; however they do not in fact cross due to the effects of spin-orbit coupling (Fig. 2). Examination of the predicted energy bands in Fig. 2 shows a flat band and small gap occurring at about 0.3 eV below the Fermi level may well account for the hump detected at this energy position in the TED curve along the $<10\bar{1}0>$.

CONCLUSION

While the data presented here is quite preliminary deviations of field emission response from that predicted by classical FN theory do occur in Re as well as W, Mo and Cu. Classical FN field emission theory does not appear to be sufficient to explain the data obtained from the $<10\bar{1}0>$ and possibly the $<0001>$ directions of rhenium. Since the calculated energy bands for rhenium cross near the Fermi level along the $<10\bar{1}0>$ direction, it is likely that the observed structure in the TED is due to band structure phenomena. Directions investigated in which there were no predicted band crossings near the Fermi level agree with classical FN theory. The

TED from the <0001> direction of Re appears normal, however, FN analysis of the data shows an inconsistency which may be attributed to an unusually large facet on this plane. While it is possible to roughly correlate anomalous TED and FN results to predicted band structure effects, further theoretical and experimental work is clearly required.

REFERENCES

1. L. Swanson, et al., Final Report, Contract NASw-1082, Field Emission Corporation. (1966) and L. W. Swanson and L. C. Crouser, Phys. Rev. 163, 622 (1967).

2. L. Swanson, et al., Final Report, Contract NASw 1516, Field Emission Corporation (1967) and L. W. Swanson and L. C. Crouser, Phys. Rev. Letters 19, 1179 (1967).

3. R. Whitcutt and B. Blott, Phys. Rev. Letters 23, No. 12, 639 (1969).

4. R. Stratton, Phys. Rev. 113, 110 (1959).

5. F. Itskovitch, Soviet Phys. JETP 23, 945 (1966); 25, 1143 (1967).

6. J. Gadzuk, to be published.

7. L. Mattheiss, Phys. Rev. 151, No. 2, 450 (1966).

8. R. Young and C. Kuyatt, Rev. Sci. Ins. 39, No. 10, 1477 (1968).

9. W. Reed, E. Fawcett, and R. Soden, Phys. Rev. 139, No. 5A, A1557 (1965).

10. L. Testardi and R. Soden, Phys. Rev. 158, No. 3, 581 (1967).

11. B. Segal, Phys. Rev. 125, No. 1, 109 (1962).

12. G. Burdick, Phys. Rev. 129, No. 1, 138 (1963).

13. A. Joseph and A. Thorsen, Phys. Rev. 133, No. 6A, A 1546 (1964).

14. A. Thorsen, A. Joseph, and L. Valby, Phys. Rev. 150, No. 2, 523 (1966).

15. E. Müller, J. Appl. Phys. 26, No. 6, 732 (1955).

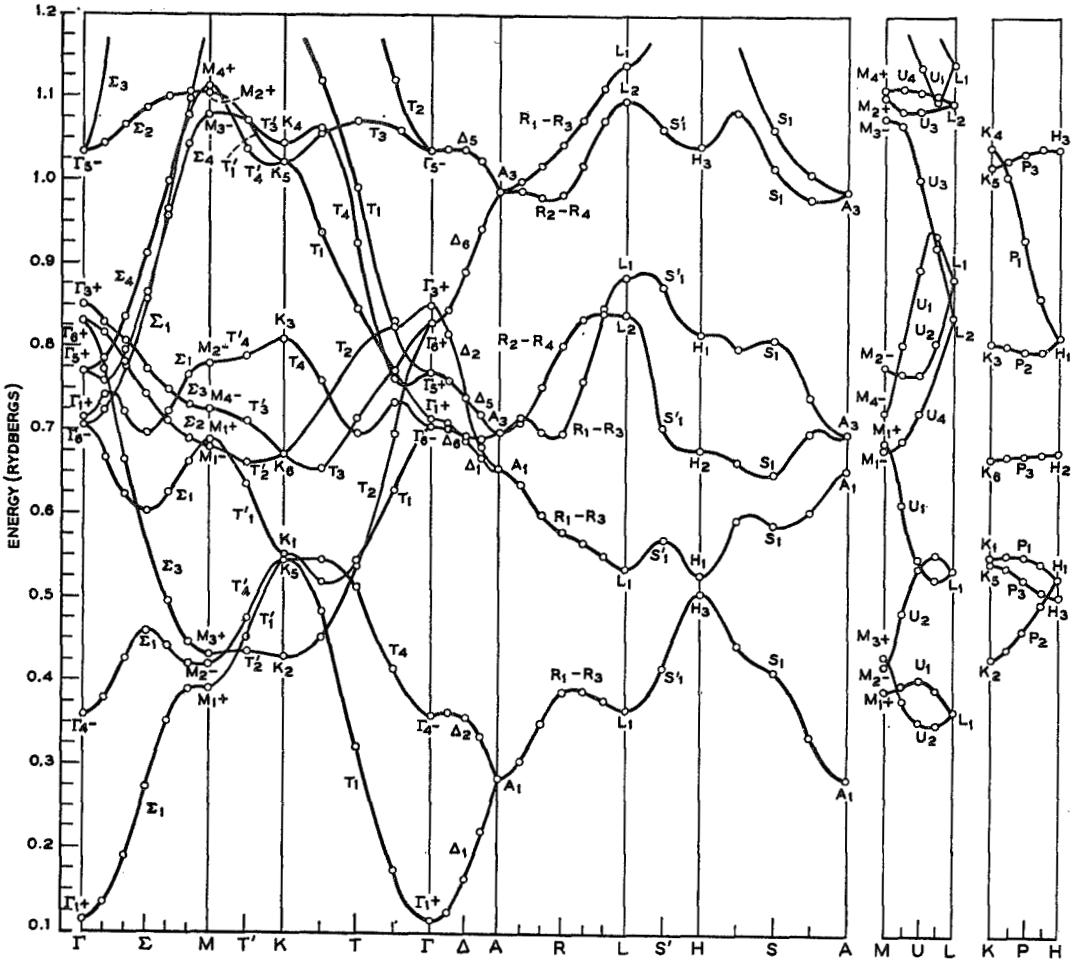

Figure 1 Relativistic energy bands for rhenium with spin-orbit coupling neglected calculated by Mattheiss[6].

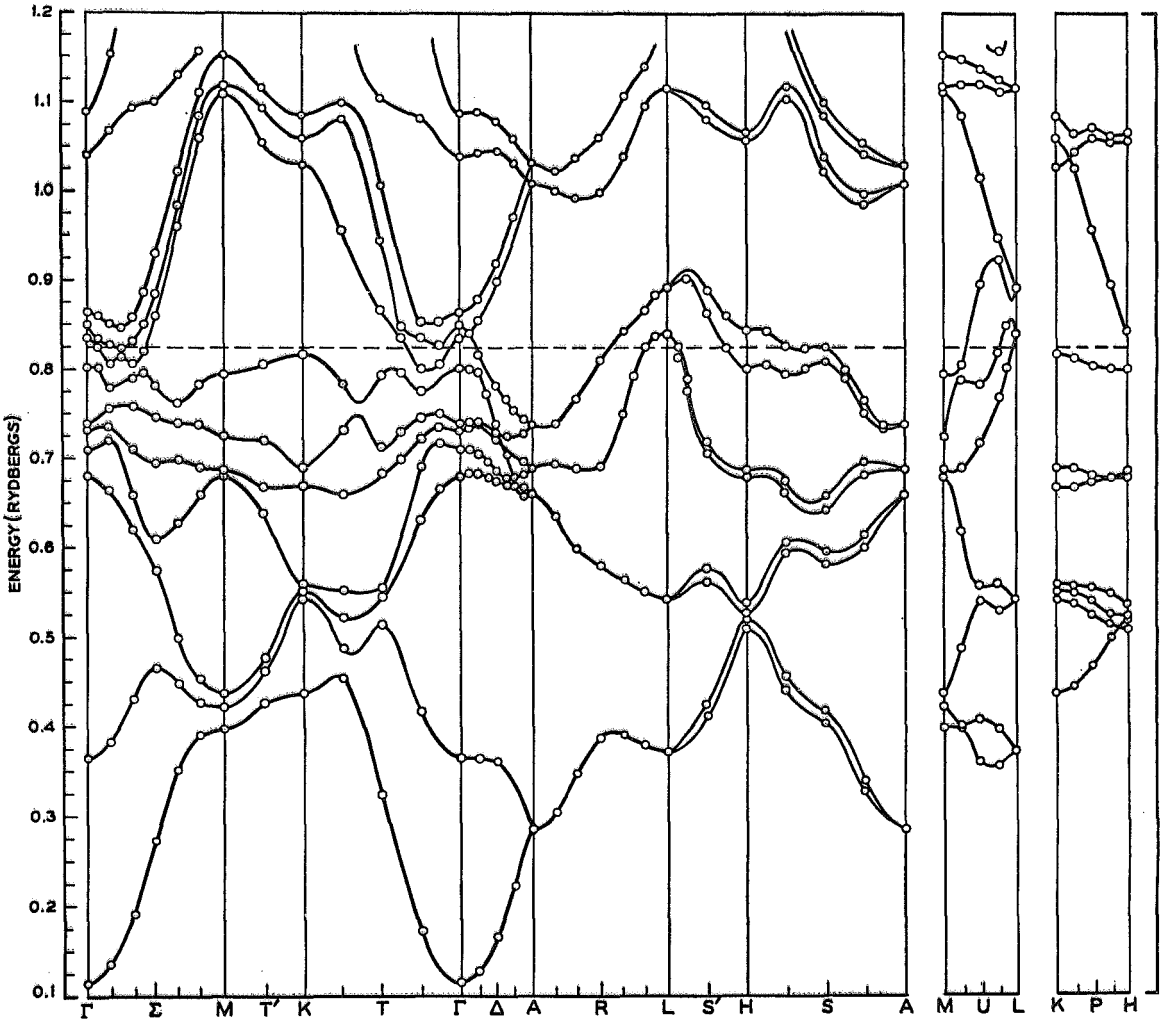

Figure 2 Relativistic energy bands for rhenium including the effects of spin-orbit coupling calculated by Mattheiss[6].

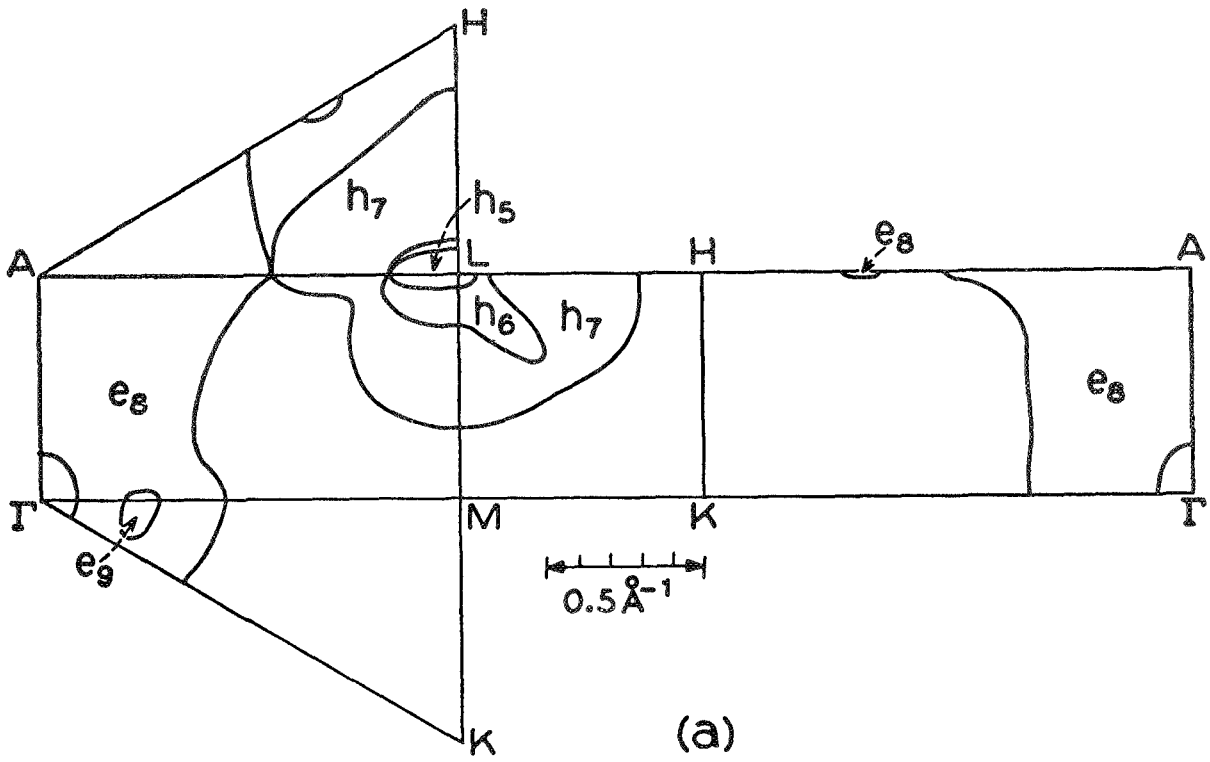

Figure 3 Intersection of the rhenium Fermi surface with symmetry planes of the hexagonal Brillouin zone according to Mattheiss[6]. The labeling denotes electrons (e) or holes (h) and the zone number.

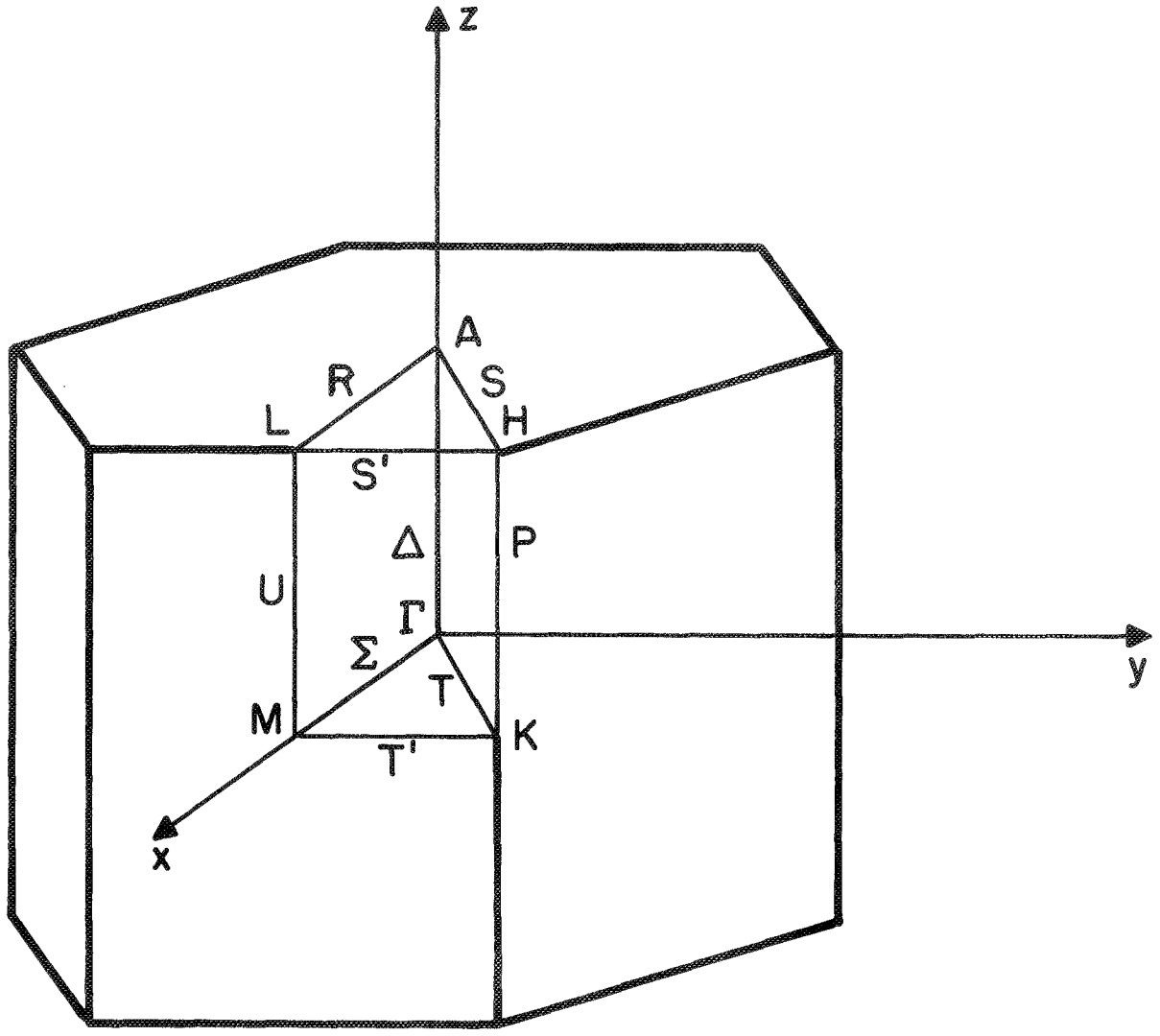

Figure 4 The Brillouin zone for the hexagonal structure with symmetry points and lines labeled according to the standard notation.

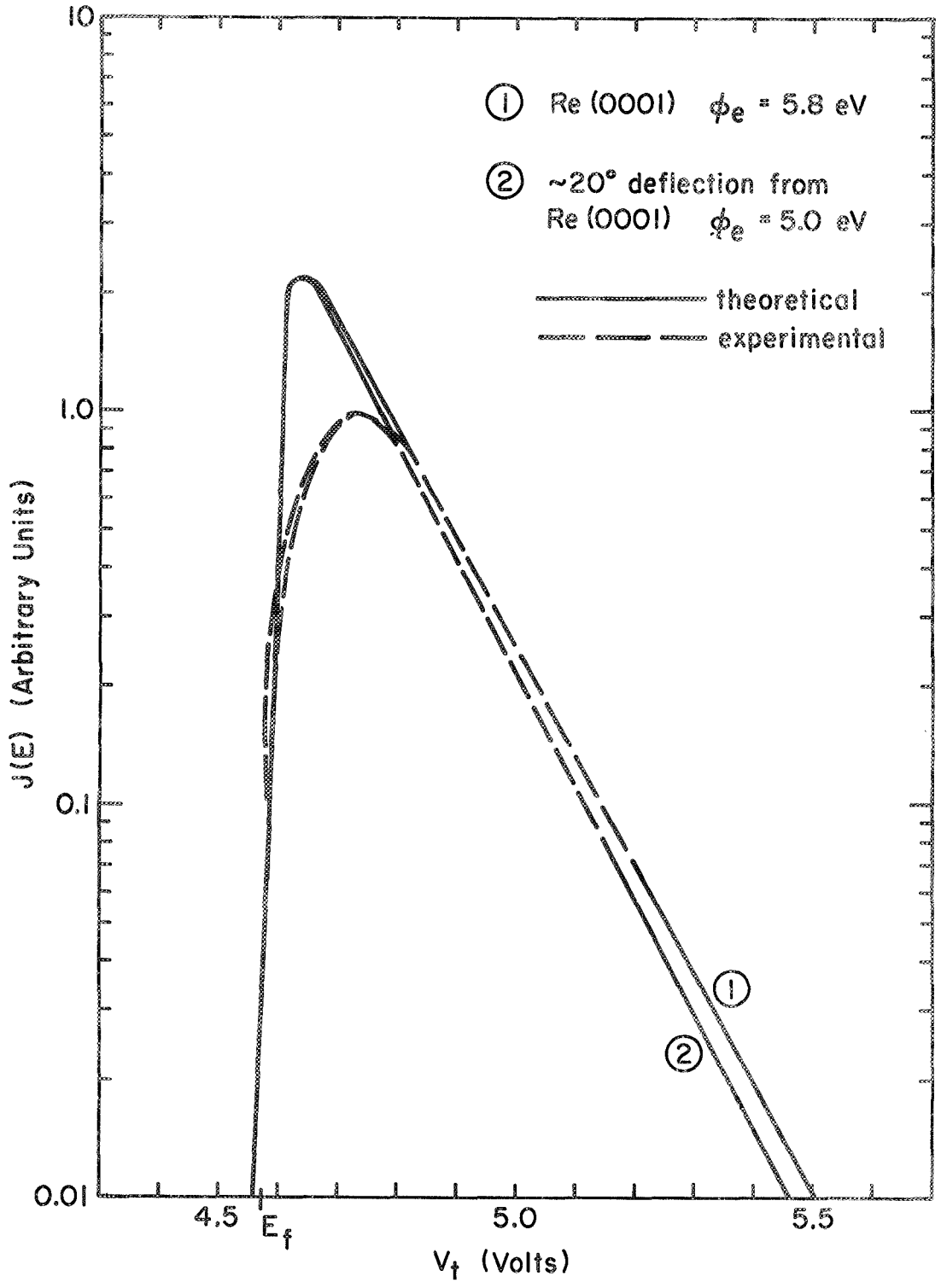

Figure 5 TED plot from (0001) of rhenium and a TED plot 20° from (0001). Note onset of emission is the same for both cases.

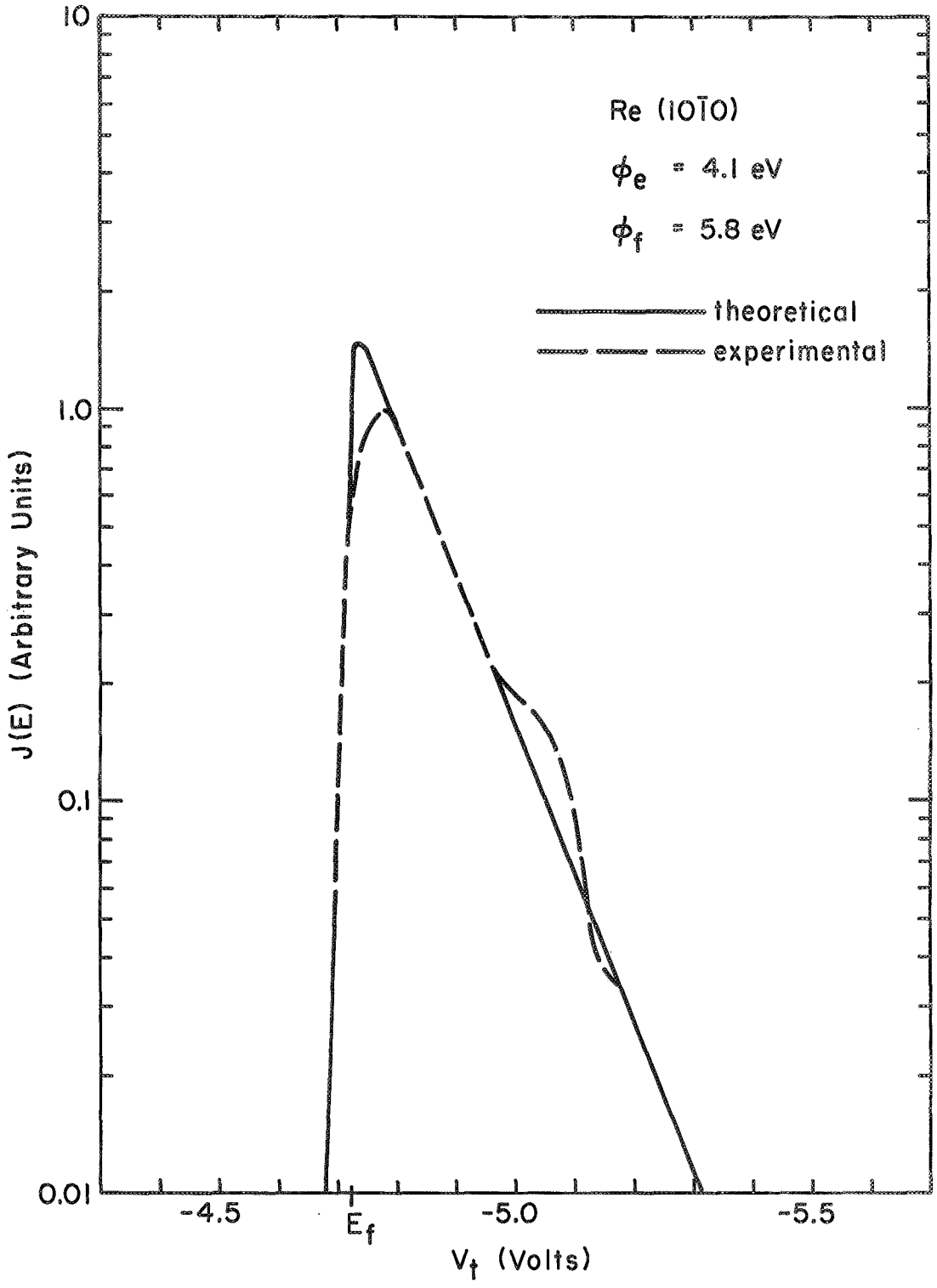

Figure 6 TED plot from (10$\bar{1}$0) of rhenium. Note hump at low energy end of plot.